Copy
RM E56L05





NACA

# RESEARCH MEMORANDUM

## HIGH-ALTITUDE PERFORMANCE OF J71-A-11 TURBOJET ENGINE AND ITS COMPONENTS USING JP-4 AND GASEOUS-HYDROGEN FUELS

By Ivan D. Smith and Martin J. Saari

Lewis Flight Propulsion Laboratory
Cleveland, Ohio





NATIONAL ADVISORY COMMITTEE
FOR AERONAUTICS

WASHINGTON

May 29, 1957





SECRET

NATIONAL ADVISORY COMMITTEE FOR AERONAUTICS

RESEARCH MEMORANDUM

# HIGH-ALTITUDE PERFORMANCE OF J71-A-11 TURBOJET ENGINE AND ITS COMPONENTS USING JP-4 AND GASEOUS-HYDROGEN FUELS

By Ivan D. Smith and Martin J. Saari

## SUMMARY

As part of an investigation of the J71-A-11 (600-B36) turbojet engine conducted in an altitude wind tunnel, data were obtained to determine the component and over-all engine performance up to the altitude limit imposed by the use of MIL-F-5624A, grade JP-4, fuel. These data were then extended to higher altitudes by the use of gaseous-hydrogen fuel.

Engine operation with JP-4 fuel at a flight Mach number of 0.8 was satisfactory up to an altitude of about 60,000 to 65,000 feet, and engine operation with marginal combustion stability was maintained up to an altitude of about 80,000 feet. The use of gaseous-hydrogen fuel provided satisfactory engine operation up to the facility operating limit of about 89,000 feet.

Operation with JP-4 fuel at an altitude of 80,000 feet, a flight Mach number of 0.8, and rated engine conditions resulted in a decrease in net thrust of 21.5 percent and an increase in specific fuel consumption of 26 percent from the values that would have been obtained had there been no loss in the performance of the components with altitude. When using gaseous-hydrogen fuel at the same operating conditions, the net thrust was approximately 4 percent greater than that obtained with JP-4 fuel because of the increased gas constant of the gaseous-hydrogen exhaust products. The specific fuel consumption with gaseous-hydrogen fuel was about 60 percent lower than that with JP-4 fuel, primarily because of the higher heating value of hydrogen.

## INTRODUCTION

The requirement that military aircraft fly higher and farther has led to investigations of the performance of turbojet engines up to the altitude limits imposed by the combustion of hydrocarbon fuels. As a means of further meeting this requirement, the altitude and range limits imposed by hydrocarbon fuels are being extended by the use of higher

energy fuels. Reference 1 indicates the theoretical gains possible when using liquid-hydrogen fuel in several engine and aircraft types. The experimental results when using hydrogen fuel in two current turbojet engines are described in reference 2.

As part of an investigation of the J71-A-11 (600-B36) turbojet engine conducted in an altitude wind tunnel at the NACA Lewis laboratory, data were obtained to determine the component and over-all engine performance up to the maximum altitude permitted by the combustion limits of MIL-F-5624A, grade JP-4, fuel. The performance evaluation was extended to the facility altitude limit (about 89,000 ft) by the use of gaseous-hydrogen fuel. Engine operating limits, compressor stall limits, and component and over-all engine performance are presented herein for the range of altitude conditions investigated with each of the fuels. The data are also presented in a form to permit computation of engine and component performance at operating conditions other than those specifically investigated, and the method of such computation is illustrated.

## APPARATUS

### Engine

The J71-A-11 (600-B36) turbojet engine has a length of $191\frac{3}{8}$ inches, a maximum height of $47\frac{5}{8}$ inches, and a maximum width of $39\frac{1}{2}$ inches. The frontal area based on the compressor tip diameter is 6.12 square feet. The dry weight of the engine and its accessories is about 4450 pounds. The manufacturer's static sea-level military performance rating is 9700 pounds of thrust with a specific fuel consumption of 0.88 pound per hour per pound of thrust at an engine speed of 6100 rpm and a turbine-outlet temperature of $1150^{\circ}$ F.

The engine control schedules the compressor acceleration bleeds to be open, the inlet guide vanes to be closed, and the exhaust nozzle to be open at engine speeds below 5300 rpm. At 5300 rpm, the compressor acceleration bleeds close, the inlet guide vanes open, and the exhaust nozzle begins to close according to a predetermined schedule with engine speed. During this investigation, however, the inlet guide vanes, compressor acceleration bleeds, and the exhaust nozzle were independently controlled. The compressor acceleration bleed ports were closed for all data reported herein.

The J71-A-11 turbojet engine has several minor airflow bleeds. These include the compressor acceleration bleed that was discharged overboard, the mid-frame and aft-frame vent flows that were seal leakages and discharged overboard, and the turbine cooling air bled from the outlet of the compressor and discharged between the turbine wheels where it reentered the main airstream. The mid-frame, aft-frame, and turbine cooling

airflows amounted to 1.4±0.4, 1.6±0.5, and 1.4±0.2 percent, respectively, of the inlet airflow.

## Engine Components

Compressor. - The J71-A-11 (600-B36) turbojet engine has a 16-stage axial-flow compressor equipped with eighth-stage acceleration bleeds and two-position inlet guide vanes. The compressor has a constant tip diameter of 33.5 inches. The hub-tip radius ratio of the first stage is 0.55 and of the last stage is 0.90. The compressor was designed to deliver an airflow of 160 pounds per second and a total-pressure ratio of 9.0 at static sea-level military conditions.

Combustor. - The combustor is a cannular type with 10 circular through-flow inner liners. JP-4 fuel is supplied to each of the 10 liners by single inlet duplex fuel nozzles. When gaseous hydrogen was used, the fuel was supplied to each liner by a tube with a 1/4-inch inside diameter discharging in the same position within the combustor as the JP-4 fuel system. Ignition was provided by two spark plugs located in diametrically opposite liners.

Turbine. - The three-stage turbine has a constant tip diameter of 33.5 inches. The hub-tip radius ratios of the first, second, and third stages are 0.795, 0.746, and 0.697, respectively.

Exhaust system. - The standard J71-A-11 exhaust system consists of a tailpipe and a continuously variable iris-type exhaust nozzle. Inasmuch as the minimum static pressure obtainable in the tunnel test section corresponds to an altitude of about 75,000 feet, an exhaust diffuser system was used to simulate engine operation at higher altitudes (see fig. 1). The diffuser, which replaced the standard tailpipe and exhaust nozzle, was designed to decelerate efficiently the exhaust gases from the turbine-outlet Mach number of about 0.55 to a diffuser-outlet Mach number of about 0.20. Thus, in contrast to a choked exhaust nozzle where the total pressure is about twice the exhaust static pressure, the diffuser-exit total and static pressures are nearly equal. By matching the diffuser-exit static pressure with the minimum obtainable test-section static pressure, the turbine-outlet total pressure for a given tunnel altitude pressure and engine operating condition can be reduced to about one-half of that required with the standard exhaust system. Therefore, at a particular engine total-pressure ratio the engine-inlet pressure can be reduced, which in this investigation amounted to an equivalent increase in altitude of about 15,000 feet above that obtainable when using the standard exhaust system with the exhaust nozzle barely choked. Variation of turbine-outlet temperature at constant engine speed was accomplished by adjusting the large butterfly valve installed near the diffuser outlet.

## Installation

The engine was mounted on a wing section that spanned the 20-foot-diameter test section of the altitude wind tunnel (fig. 1). Dry air at pressures and temperatures giving the desired engine-inlet Reynolds number indices was ducted to the engine inlet through a venturi used to measure airflow. When using the standard engine exhaust system (fig. 2), thrust measurements by the tunnel balance scales were made possible by a frictionless slip joint in the engine-inlet duct. Scale thrust measurements were, of course, meaningless when the high-altitude tailpipe (exhaust diffuser) was used.

## Instrumentation

The instrumentation for measuring pressures and temperatures was installed at various stations throughout the engine as shown in figure 2. The table presented on the figure indicates the number and type of measurements at each station. The total-pressure and temperature probes at each station were located at the centers of equal annular area increments so that measurements could be averaged arithmetically. Instrumentation was also provided to measure the airflow at the mid-frame and aft-frame vents and in the turbine cooling duct.

The pressures were measured by null-type diaphragm capsules and recorded by a digital automatic multiple pressure recorder. The temperatures were measured and recorded by iron-constantan or chromel-alumel thermocouples in conjunction with an automatic digital potentiometer. One feature of particular importance is the design of the thermocouples used to measure exhaust-gas temperatures. The radiation error of a thermocouple installed in a hot-gas stream where the gas temperature is considerably higher than the wall temperature becomes substantial at very low pressures (ref. 3). For example, at a tailpipe total pressure of 200 pounds per square foot absolute shielded nonaspirated thermocouples indicated a gas temperature 75° F lower than the true temperature. Properly shielded and aspirated thermocouples, as described in reference 3, were used to minimize the radiation error.

The flow rate of JP-4 fuel was measured by rotameters and that of gaseous hydrogen by calibrated orifices. When using the standard exhaust system, the exhaust-nozzle area was obtained from a calibrated indicator mounted on the nozzle actuator. The calibration of this indicator with exhaust-nozzle area was made with the nozzle cold.

## PROCEDURE

During the investigation of the J71-A-11 turbojet engine steady-state data were taken over a range of engine speeds from the lowest operable

speed to a rated speed of 6100 rpm and effective exhaust-nozzle areas from the largest obtainable area to the area producing the limiting turbine-outlet temperature, 1190° F, at each of the following compressor-inlet Reynolds number indices:

| Standard engine exhaust system | High-altitude exhaust system | |
|---|---|---|
| JP-4 fuel | JP-4 fuel | Hydrogen fuel |
| 0.275, 0.44, 0.65 | 0.05, 0.06, 0.08, 0.10, 0.15, 0.20, 0.30 | 0.035, 0.04, 0.05, 0.06 |

Altitudes and flight Mach numbers associated with these Reynolds number indices (assuming 100-percent ram-pressure recovery) may be determined from figure 3. The ambient static pressure was maintained at certain altitude values when using the standard engine exhaust system and was held at the lowest value possible when using the high-altitude system. Data obtained with the standard exhaust system were used to define the exhaust-system pressure losses and the exhaust-nozzle velocity coefficient for use in calculating engine performance from pumping characteristics. The inlet guide vanes were open and the compressor acceleration bleeds closed for all data taken.

The stall limits of the compressor were determined by a series of increasing fuel steps at several Reynolds number indices.

The fuels used during this investigation were MIL-F-5624A, grade JP-4, which has a lower heating value of 18,700 Btu per pound and a hydrogen-carbon ratio of 0.171, and gaseous hydrogen, which has a lower heating value of 51,570 Btu per pound and a purity of 98 percent.

Definitions of symbols, methods of calculation, and a sample calculation of performance from generalized performance data are presented in appendixes A, B, and C, respectively.

## RESULTS AND DISCUSSION

### Altitude Operating Limits

The altitude operating limits of the J71-A-11 turbojet engine are presented in figure 4 for a flight Mach number of 0.8. When using JP-4 fuel, satisfactory engine operation was attained up to an altitude of 60,000 to 65,000 feet, and engine operation with marginal combustion could be maintained up to an altitude of about 80,000 feet. Satisfactory engine operation was obtained up to the facility limit of about 89,000 feet when operating with gaseous-hydrogen fuel. Furthermore, combustor blowout was not encountered at any altitude even during compressor surge conditions.

At lower engine speeds, engine operation with bleeds closed was limited by compressor stall. The minimum stall-limited engine speed increased from 4570 rpm at an altitude of 60,000 feet to 5030 rpm at an altitude of 88,000 feet.

## Component Performance

The over-all performance of each component is presented to aid in the understanding of engine operation at the higher altitudes. An attempt has been made to present the performance of each component in such a manner that the relationship between its operating point and the over-all engine operating point can be determined. Generalized component performance is presented over the complete range of high-altitude operating conditions investigated, and performance maps are presented at certain selected operating conditions. Trends of component performance at altitudes lower than those investigated herein are presented in reference 4.

Generalized performance. - The knowledge of turbine-inlet temperature is important in turbine performance and also in compressor-turbine matching. Since over-all engine performance is usually given in terms of a turbine-outlet temperature, the relation between turbine-inlet and -outlet temperatures is given in figure 5. This relation is valid within ±1 percent for the range of compressor-inlet Reynolds number index investigated and for both JP-4 and gaseous-hydrogen fuels. Both turbine-inlet and -outlet temperatures are presented as ratios to compressor-inlet temperature for convenience in using other figures presented herein.

Compressor: Theoretical analysis shows that the difference in properties of the two fuels being considered affects turbine performance and, therefore, compressor-turbine matching. The rematching that occurs when burning gaseous-hydrogen fuel results from (1) a lower fuel mass addition, (2) a lower turbine-inlet temperature required to maintain turbine work output because of the increase in specific heat of the combustion products, and (3) an increase in turbine-inlet pressure (and compressor-exit pressure) because of the increase in gas constant. The combined effect tends to increase compressor pressure ratio at a given corrected engine speed. This change in compressor pressure ratio, however, is small, about 1 percent, and, consequently, no change can be discerned from the experimental data. Compressor performance can, therefore, be considered identical during operation with either fuel.

For a given compressor-inlet Reynolds number index, the corrected airflow (in the high engine speed region) and compressor efficiency are essentially functions of corrected engine speed. The corrected airflow and efficiency of the J71-A-11 compressor are presented in figures 6(a) and (b) for several constant corrected engine speeds over the range of compressor-inlet Reynolds number index investigated. A change in compressor-inlet Reynolds number index from 0.30 to 0.035 reduced corrected airflow by about 17 percent and compressor efficiency by 7.5 points

at each of the corrected engine speeds shown. The greatest portion of the losses occurred at Reynolds number indices below about 0.15.

In order to determine compressor performance at flight conditions other than those specifically investigated, it is necessary to define the relation between compressor pressure ratio and compressor-inlet Reynolds number index. Since compressor pressure ratio is a function of turbine-inlet temperature, as indicated by the turbine corrected weight-flow equation for choked flow, the compressor pressure ratio parameter $\frac{P_2/P_1}{\sqrt{T_4/T_1}}$ can be utilized. The variation of the pressure ratio parameter with compcompressor-inlet Reynolds number is shown in figure 6(c) for several constant corrected engine speeds. A change in Reynolds number index from 0.30 to 0.035 resulted in a 12-percent reduction in the pressure ratio parameter. Here again, as with airflow and efficiency, most of the reduction occurred at Reynolds number indices below 0.15. Thus, with the relations of corrected compressor airflow, efficiency, and pressure ratio parameter with Reynolds number index defined, it is possible to estimate compressor performance at any flight condition within the range investigated.

The compressor stall limits are shown in figure 6(d) for a range of altitudes at a flight Mach number of 0.8. The approximate steady-state region and the military rated engine operating points for the same range of altitudes are also presented. The steady-state operating lines could not be shown because the exhaust-nozzle schedule had not been fixed. At a corrected engine speed of 6100 rpm, the maximum compressor pressure ratio obtainable without encountering stall varied from 9.9 at 40,000 feet to 8.7 at 80,000 feet. The engine speed at which the stall line and steady-state operating lines intersect increases with altitude as was specifically shown in figure 4.

Combustor: The variation of combustion efficiency with the combustion parameter $w_{a,3}T_6$ is shown in figure 7. The more conventional combustion generalization parameter $P_2T_2/V_3$ is shown as a second scale. The combustor reference velocity $V_3$ was 98.5 feet per second. Combustion efficiency for JP-4 fuel decreased at nearly a uniform rate from 0.99 to 0.90 as $w_{a,3}T_6$ was decreased from 150,000 to 13,000. Further reduction in $w_{a,3}T_6$ resulted in a more rapid decrease in combustion efficiency. At a $w_{a,3}T_6$ of 7500 the combustion efficiency had decreased to about 0.76, and the combustion was very near the blowout limit.

Because of the difficulty in measuring the flow rate of gaseous-hydrogen fuel, a considerable amount of data scatter exists in the combustion efficiency. Data indicate, however, that a combustion efficiency of approximately 0.80 was obtained in the $w_{a,3}T_6$ range from 13,000 to 6000.

When operating at corrected engine speeds from 5500 to 6600 rpm and engine temperature ratios from 2.5 to 3.5, the approximate range of $w_{a,3}T_6$ at each compressor-inlet Reynolds number index investigated was:

| Compressor-inlet Reynolds number index, $\delta_1/\varphi_1\sqrt{\theta_1}$ | Combustion parameter, $w_{a,3}T_6 \times 10^{-3}$, (lb)($^{\circ}$R)/sec | Compressor-inlet Reynolds number index, $\delta_1/\varphi_1\sqrt{\theta_1}$ | Combustion parameter, $w_{a,3}T_6 \times 10^{-3}$, (lb)($^{\circ}$R)/sec |
|---|---|---|---|
| 0.65 | 100 - 160 | 0.08 | 10 - 18 |
| .44 | 65 - 100 | .06 | 8 - 13 |
| .30 | 40 - 70 | .05 | 6 - 10 |
| .20 | 25 - 50 | .04 | - 8 |
| .15 | 18 - 35 | .035 | - 7 |
| .10 | 13 - 25 | | |

A sample calculation for a precise determination of the value of $w_{a,3}T_6$ at any engine operating point is presented in appendix C.

The variation of combustor total-pressure loss with combustor temperature ratio is shown in figure 8. As the combustor temperature ratio increased from 1.5 to 2.3, the combustor total-pressure loss decreased from about 0.06 to 0.045 of the combustor-inlet total pressure. The reduction in combustor pressure loss with increasing combustor temperature ratio is caused by the rapid decrease in friction pressure loss that accompanies the decrease in combustor flow velocities as engine speed increases or as exhaust-nozzle area decreases. In the normal and military operating ranges of the engine a combustor total-pressure-loss ratio of 0.045 to 0.05 was encountered.

Turbine: Turbine performance is presented in figure 9 as a function of turbine-inlet Reynolds number index. The corrected turbine gas flow decreased only slightly at low Reynolds number indices and was between approximately 40 and 41 pounds per second over the entire range of conditions investigated.

At a given turbine-inlet Reynolds number index, turbine efficiency (fig. 9(b)) was essentially a function of corrected turbine speed and was independent of the fuel used. At a corrected turbine speed of 3000 rpm (near rated), turbine efficiency decreased from 0.785 to 0.710 as turbine-inlet Reynolds number index decreased from 0.37 to 0.04.

At a given turbine-inlet Reynolds number index, corrected turbine work (fig. 9(c)) was essentially a function of turbine total-pressure ratio for the small range of corrected turbine speed that can be obtained at a given total-pressure ratio when the turbine is operating in an engine.

To maintain a given corrected turbine work output the turbine total-pressure ratio had to be increased approximately 13 percent as the turbine Reynolds number index was decreased from 0.40 to 0.06. The use of gaseous-hydrogen fuel allowed a reduction in turbine total-pressure ratio of about 3 percent while still maintaining the same corrected turbine work output because of an increase in the gas constant of the combustion products.

In order to determine the turbine Reynolds number index at any given over-all engine operating point a correlation of the turbine- and compressor-inlet Reynolds number indices is presented in figure 10. At any constant compressor Reynolds number index the turbine Reynolds number index can be defined within ±3 percent by the corrected turbine speed.

Standard exhaust system: Some low-altitude data were taken with the standard J71-A-11 tailpipe and exhaust nozzle. The exhaust-system data are presented to allow calculation of standard over-all engine performance from pumping characteristics.

The variation of the tailpipe total-pressure loss with the tailpipe flow parameter $w_{g,5}\sqrt{T_9}/P_5$ is shown in figure 11(a). Since this parameter is a function of turbine-outlet Mach number, high tailpipe total-pressure losses were encountered at high values of the parameter. At any operating point in the normal or military operating range a tailpipe total-pressure loss of 2 to 4 percent of the inlet total pressure was encountered.

The exhaust-nozzle velocity coefficient is shown in figure 11(b) as a function of nozzle pressure ratio. When the exhaust nozzle was unchoked (nozzle pressure ratio $P_9/p_0 < 1.9$), sufficient data scatter made the values unreliable. When the exhaust nozzle was choked, however, data fell about a mean value of 0.985.

Performance maps. - In order to illustrate more clearly the shift in compressor and turbine operating points when changing from a low- to a high-altitude condition, operating points are shown on the selected compressor and turbine maps in figures 12 and 13, respectively. The turbine performance maps are presented for operation with both JP-4 and gaseous-hydrogen fuels at the high-altitude condition. The engine operating point that has been selected for illustration is as follows:

| | |
|---|---|
| Engine speed, N, rpm | 6100 |
| Exhaust-gas temperature, $T_6$, °F | 1200 |
| Flight Mach number, $M_0$ | 0.8 |
| Altitude (low condition), ft | 43,000 |
| Altitude (high condition), ft | 81,000 |

At the selected engine operating point the compressor pressure ratio decreased from 9.15 to 8.35 and the corrected airflow decreased from 167 to 149 pounds per second when changing from the low- to the high-altitude condition (fig. 12).

The turbine work increased when changing from the low- to the high-altitude condition at the selected operating point because of the decreased turbine efficiency and the increased work required by the compressor because of decreased compressor efficiency. When using JP-4 fuel (figs. 13(a) and (b)), the turbine pressure ratio had to be increased from approximately 3.22 to 3.75 when changing from the low- to the high-altitude condition to supply the necessary compressor work. At the high-altitude condition, the use of gaseous-hydrogen fuel reduced the turbine pressure ratio requirement to about 3.65 because of the increase in the gas constant of the exhaust products.

## Over-All Engine Performance

Over-all engine performance is presented in the same manner as the component performance in that generalized performance is presented over the complete range of operating conditions investigated, and performance maps are presented at certain selected altitude operating conditions.

Generalized performance. - Over-all engine performance is presented in terms of pumping characteristics in figures 14 and 15 for JP-4 and gaseous-hydrogen fuels, respectively. A pumping map at one compressor-inlet Reynolds number index is presented for each of the two fuels investigated together with corrections to be applied to these pumping characteristics for other Reynolds number indices over the range investigated.

The pumping maps (figs. 14(a) and 15(a)) are at compressor-inlet Reynolds number indices of 0.20 and 0.04 for JP-4 and gaseous-hydrogen fuels, respectively. These Reynolds number indices were selected because in each case the greatest range of engine speed and engine temperature ratio was obtained at these conditions. When using JP-4 fuel the range of corrected engine speed obtained was from 5000 to 6600 rpm (82 to 108 percent rated), and the range of engine temperature ratios was from 1.8 to 4.0 (fig. 14(a)). With gaseous-hydrogen fuel the corrected engine speed range was from 5400 to 6600 rpm (88.5 to 108 percent rated), and the engine temperature ratio range was from 3.2 to 4.0 (fig. 15(a)).

The pumping characteristic corrections for other compressor-inlet Reynolds number indices (figs. 14(b) and 15(b)) over the range investigated are presented as engine total-pressure ratio and corrected airflow corrections at a constant engine total-temperature ratio and corrected engine speed to be applied to the values read from the pumping maps. These engine total-pressure-ratio and airflow corrections are valid

within ±1 and ±3 percent, respectively, for all corrected engine speeds and engine temperature ratios over the range investigated. (The range of compressor-inlet Reynolds number index was from 0.05 to 0.65 when using JP-4 fuel and from 0.035 to 0.06 when using gaseous-hydrogen fuel.)

Performance maps. - Over-all engine performance maps are presented in figure 16 for the same low- and high-altitude conditions as the compressor and turbine maps previously discussed. The selected operating point discussed in connection with the compressor and turbine maps is also shown.

The performance maps indicate, in general, that for JP-4 fuel an increase in altitude caused the region of minimum specific fuel consumption to shift from the low-engine-speed - net-thrust region to the high-engine-speed - net-thrust region (figs. 16(a) and (b)). At the high-altitude condition the region of specific fuel consumption for gaseous-hydrogen fuel occurred in the intermediate-engine-speed - thrust range (fig. 16(c)). Thrust modulation from a selected operating point in the high-engine-speed range for either fuel can be most economically accomplished by variation of engine speed at a constant nozzle area rather than by variation of nozzle area at constant speed.

Because of decreases in component performance the specific fuel consumption increased from about 1.15 to 1.46 pounds per hour per pound of thrust and the exhaust-nozzle area increased from about 2.46 to 2.83 square feet when changing from the low- to the high-altitude condition and using JP-4 fuel at the selected operating point. At the high-altitude condition, the change from JP-4 to gaseous-hydrogen fuel increased the net thrust from 295 to 310 pounds and decreased the exhaust-nozzle area from about 2.83 to 2.73, both effects resulting from the improvement in turbine performance and the associated decrease in tailpipe pressure loss. The specific fuel consumption was about 60 percent lower when using gaseous-hydrogen fuel primarily because of the higher heating value. The method of performance calculations is presented in appendix C.

## Contribution of Individual Component Losses to Over-All Engine Performance Losses

In order to show more clearly how the performance loss of each component at high altitudes affects the over-all engine performance, the net thrust and specific fuel consumption obtained when incorporating each component loss separately are presented in figure 17. Data are presented for altitudes from 35,000 feet to the maximum attained at a flight Mach number of 0.8 when operating at an engine speed of 6100 rpm and an exhaust-gas temperature of 1200° F.

The loss in over-all engine performance due to reductions in component performances was negligible for altitudes up to 35,000 feet. Losses in net thrust were encountered as altitude was increased beyond an altitude of 35,000 feet primarily because of a reduction in corrected airflow and compressor and turbine efficiencies. Increases in specific fuel consumption at higher altitudes were principally due to reductions in compressor, combustor, and turbine efficiencies.

When operating at 80,000 feet the itemized altitude losses are as follows:

| Component loss | Net thrust, percent | | Specific fuel consumption, percent | |
|---|---|---|---|---|
| | JP-4 fuel | Gaseous-hydrogen fuel | JP-4 fuel | Gaseous-hydrogen fuel |
| Combustion efficiency | 0 | 0 | 11.0 | [a]16.5 |
| Corrected airflow | 11.2 | 11.2 | 0 | 0 |
| Compressor and turbine efficiencies | 9.3 | 7.3 | 13.6 | 12.5 |
| Increase in tailpipe pressure loss | 1.0 | .5 | 1.3 | .9 |
| Total loss | 21.5 | 19.0 | 25.9 | 29.9 |

[a]Assuming the combustion efficiency of hydrogen and JP-4 fuels would be the same when operating at sea-level conditions.

It should be noted that although the percentage increase in specific fuel consumption due to combustion efficiency is higher for gaseous hydrogen than for JP-4 fuel at the selected flight condition, the absolute value of specific fuel consumption is still much lower. Furthermore, reference 5 indicates that the performance of a combustor and fuel-injection system tailored for the use of gaseous-hydrogen fuel is superior to a standard JP-4 combustor configuration, particularly in the range of low combustor-inlet pressures. The increase in specific fuel consumption due to a loss in combustion efficiency with altitude for gaseous-hydrogen fuel could therefore be expected to be equal to or less than that obtained with JP-4 fuel over the entire range of flight conditions.

## Exhaust-Nozzle-Area Requirements

The effective exhaust-nozzle area required to maintain a constant exhaust-gas temperature at an engine speed of 6100 rpm is shown in figure 18 over a range of altitudes at a flight Mach number of 0.8. The effective exhaust-nozzle area increased slightly with increasing flight Mach number but was found to be within ±2 percent of the values presented over

the range of flight Mach numbers considered (0 to 1.4). The effective area of the standard exhaust nozzle for choked-flow operation was found to be 0.95±0.02 of the actual exhaust-nozzle area (calibrated cold).

Effective exhaust-nozzle area decreased with an increase in altitude up to 35,000 feet because of decreased engine-inlet temperature. At altitudes above 35,000 feet, inlet temperature remained constant but the decrease in component efficiencies required increased exhaust-nozzle area.

If a fixed-area exhaust nozzle were used and sized at sea level using JP-4 fuel, rated engine speed operation would not be possible above an altitude of 50,000 feet with JP-4 fuel and above about 65,000 feet with gaseous-hydrogen fuel without causing turbine overtemperature. The exhaust-nozzle-area variation required at a constant exhaust-gas temperature when operating from sea level to 80,000 feet with JP-4 fuel was about 0.96 to 1.17 of the sea-level exhaust-nozzle area. The use of gaseous-hydrogen fuel allows approximately a 6-percent reduction in exhaust-nozzle area because of the reduction in required turbine pressure ratio and the resultant reduction in tailpipe pressure loss.

### Altitude Performance at Rated Engine Conditions

The net thrust, fuel flow, and airflow of the J71-A-11 turbojet engine are shown in figures 19 and 20 over the range of altitudes and flight speeds investigated when operating at three constant exhaust-gas temperatures (1100°, 1200°, and 1300° F) and an engine speed of 6100 rpm. Data are shown for both JP-4 and gaseous-hydrogen fuels. These curves are presented primarily to show absolute levels of engine performance over a wide range of altitude conditions when operating at rated engine speed and do not show any important trends not previously discussed.

## CONCLUDING REMARKS

At a flight Mach number of 0.8, the J71-A-11 turbojet engine operated satisfactorily on JP-4 fuel up to an altitude of about 60,000 to 65,000 feet, and engine operation with marginal combustion was obtained up to an altitude of about 80,000 feet. When operating with gaseous-hydrogen fuel, satisfactory engine operation was attained up to the facility operating limit of about 89,000 feet.

An increase in altitude from 43,000 to 88,000 feet at a flight Mach number of 0.8 (compressor-inlet Reynolds number indices from 0.30 to 0.035) decreased both compressor and turbine efficiencies about 7.5 points and decreased corrected airflow about 17 percent. When operating at rated engine conditions at the altitude limit imposed by the use of JP-4 fuel (about 80,000 ft at a flight Mach number of 0.8), combustion efficiency

decreased about 11 points from that obtained at conditions where there was no altitude effect. This loss, in combination with the decreased compressor and turbine efficiencies and corrected airflow, resulted in a 21.5-percent reduction in net thrust and an increase in specific fuel consumption of approximately 26 percent in comparison with the values that would be obtained assuming no loss in component performance with altitude.

Net thrust was approximately 4 percent higher when operating with gaseous-hydrogen fuel than with JP-4 fuel because of the decreased turbine total-pressure drop due to the higher gas constant of the combustion products and the resultant decrease in tailpipe total-pressure loss. Specific fuel consumption was about 60 percent lower when using gaseous-hydrogen fuel, primarily because of the increased heating value.

Lewis Flight Propulsion Laboratory
National Advisory Committee for Aeronautics
Cleveland, Ohio, December 11, 1956

# APPENDIX A

## SYMBOLS

The following symbols are used in this report:

| | |
|---|---|
| A | area, sq ft |
| C | coefficient |
| F | thrust, lb |
| g | acceleration due to gravity, 32.17 $ft/sec^2$ |
| H | enthalpy, Btu/lb |
| M | Mach number |
| N | engine speed, rpm |
| P | total pressure, lb/sq ft abs |
| p | static pressure, lb/sq ft abs |
| R | gas constant, ft-lb/(lb)($^oR$) |
| T | total temperature, $^oR$ |
| t | static temperature, $^oR$ |
| V | velocity, ft/sec or knots |
| w | flow rate, lb/sec or lb/hr |
| $\beta$ | $\gamma$ correction factor; $\beta = \frac{1.4}{\gamma} \frac{\left(\frac{\gamma + 1}{2}\right)^{\frac{\gamma}{\gamma-1}}}{\left(\frac{1.4 + 1}{2}\right)^{\frac{1.4}{1.4-1}}}$ |
| $\gamma$ | ratio of specific heats |

$\delta$ ratio of total pressure to NACA standard sea-level static pressure

$\delta/\varphi\sqrt{\theta}$ Reynolds number index

$\eta$ efficiency

$\theta$ ratio of total temperature to NACA standard sea-level static temperature

$\varphi$ ratio of absolute viscosity to viscosity of NACA standard atmosphere at sea level

Subscripts:

a air

ab acceleration bleed

av aft-frame vent

b combustor

c compressor

eff effective

f fuel

g gas

id ideal

j jet

mv mid-frame vent

n net

s scale

t turbine

tc turbine cooling

v velocity

x slip joint in inlet duct

| | |
|---|---|
| 0 | free-stream conditions |
| 1 | compressor inlet |
| 2 | compressor outlet |
| 3 | combustor inlet |
| 4 | combustor outlet, turbine inlet |
| 5 | turbine outlet (standard engine exhaust system) |
| 5a | turbine outlet (high-altitude tailpipe) |
| 6 or 6a | tailpipe outlet (high-altitude tailpipe) |
| 9 | exhaust-nozzle inlet (standard engine exhaust system) |
| 10 | exhaust-nozzle throat (standard engine exhaust system) |

# APPENDIX B

## METHODS OF CALCULATION

### Airflow

The engine-inlet airflow $w_{a,1}$ was calculated from one-dimensional compressible-flow relations (ref. 6) using the area and the average pressures and temperatures at a venturi in the inlet-air duct. Air bleeds and the addition of fuel resulted in the following mass flows at other stations:

$$w_{a,2} = w_{a,1} - w_{a,ab}$$

$$w_{a,3} = w_{a,2} - w_{a,tc} - w_{a,mv} - w_{a,av}$$

$$w_{g,4} = w_{a,3} + w_f/3600$$

$$w_{g,6} = w_{g,4} + w_{a,tc}$$

$$w_{g,9} = w_{g,6}$$

### Compressor Efficiency

The compressor efficiency is defined as the ratio of isentropic enthalpy rise to the actual enthalpy rise across the compressor:

$$\eta_c = \frac{H_{a,2,isentropic} - H_{a,1}}{H_{a,2} - H_{a,1}}$$

The enthalpy values were determined from charts based on the material of reference 7 and using variable specific heats.

### Combustion Efficiency

The combustion efficiency is defined as the ratio of the ideal fuel-air ratio necessary to obtain the engine temperature rise to the actual fuel-air ratio:

$$\eta_b = \frac{w_f/w_{a,5,id}}{w_f/w_{a,5,actual}}$$

The ideal fuel-air ratio was determined from the fuel properties and the engine temperature rise (see fig. 21 or ref. 8).

### Turbine Efficiency

The turbine efficiency is defined as the ratio of actual enthalpy drop to isentropic enthalpy drop across the turbine:

$$\eta_t = \frac{H_{g,4} - H_{g,5}}{H_{g,4} - H_{g,5,\text{isentropic}}}$$

The turbine-inlet temperature $T_4$ was calculated by assuming that the turbine enthalpy drop equaled the compressor enthalpy rise. The turbine-outlet temperature $T_5$ was calculated from the measured value of $T_6$ by accounting for the temperature drop between the two stations caused by the turbine cooling air.

The enthalpy values were then determined from charts based on the material of reference 7 and using variable specific heats.

### Scale Jet Thrust

Scale jet thrust was determined when using the standard engine exhaust system by an algebraic summation of the forces acting on the engine:

$$F_{j,s} = F_B + F_D + \frac{w_{a,1}}{g} V_x + A_x(p_x - p_0)$$

where $F_B$ is the force due to the balance scale, $F_D$ is the external drag of the installation, and the last two terms represent the momentum and pressure forces on the installation at the slip joint in the inlet-air duct.

### Calculated Thrust

Jet thrust was calculated from the gas flow and the effective velocity:

$$F_j = \frac{w_{g,9}}{g} C_v V_{eff}$$

The effective velocity, which includes the effect of excess pressure not converted to velocity for supercritical pressure ratios, was obtained from the effective velocity parameter of reference 6 (see also fig. 23).

## APPENDIX C

## SAMPLE CALCULATION OF PERFORMANCE FROM GENERALIZED PERFORMANCE DATA

In order to illustrate the method for obtaining component and overall engine performance from generalized performance data, a numerical example is presented for the following flight and engine conditions:

| | |
|---|---|
| Altitude, ft | 80,000 |
| Flight Mach number, $M_0$ | 0.8 |
| Engine speed, N, rpm | 6100 |
| Exhaust-gas temperature, $T_6$, $^{\circ}R$ | 1660 |

From this the following quantities are known:

$$p_0 = 58.0 \text{ lb/sq ft abs}$$

$$t_0 = 392.4^{\circ} \text{ R}$$

From these quantities and assuming 100-percent ram-pressure recovery and an NACA standard day, the following parameters may be calculated:

$$V_0 = 777 \text{ ft/sec}$$

$$P_1 = 88.4 \text{ lb/sq ft abs}$$

$$T_1 = 442.6^{\circ} \text{ R}$$

$$\sqrt{\theta_1} = 0.9235$$

$$\delta_1 = 0.0418$$

$$\delta_1/\varphi_1\sqrt{\theta_1} = 0.0520$$

$$N/\sqrt{\theta_1} = 6605 \text{ rpm}$$

$$T_6/T_1 = 3.75$$

To illustrate the major performance differences when using JP-4 and gaseous-hydrogen fuels, the sample calculation will be shown for both fuels.

From figures 14(a) and 15(a) the following values may be obtained at the base Reynolds number indices:

| | JP-4 fuel | Gaseous hydrogen |
|---|---|---|
| $(P_5/P_1)_{base}$ = | 2.64 | 2.11 |
| $(w_{a,1}\sqrt{\theta_1}/\delta_1)_{base}$ = | 166.1 lb/sec | 142.5 lb/sec |

Since the flight condition selected is not at the base Reynolds number index, the following corrections to these parameters are necessary:

From figures 14(b) and 15(b):

| | JP-4 fuel | Gaseous hydrogen |
|---|---|---|
| $\frac{P_5/P_1}{(P_5/P_1)_{base}}$ = | 0.806 | 1.051 |
| $\frac{w_{a,1}\sqrt{\theta_1}/\delta_1}{(w_{a,1}\sqrt{\theta_1}/\delta_1)_{base}}$ = | 0.892 | 1.040 |

Multiplying by the corrections, the engine total-pressure ratio and corrected airflow can be obtained for the proper Reynolds number index:

| | JP-4 fuel | Gaseous hydrogen |
|---|---|---|
| $P_5/P_1$ = | 2.128 | 2.218 |
| $w_{a,1}\sqrt{\theta_1}/\delta_1$ = | 148.2 lb/sec | 148.2 lb/sec |

and

| | | |
|---|---|---|
| $P_5$ = | 188 lb/sq ft abs | 196 lb/sq ft abs |
| $w_{a,1}$ = | 6.71 lb/sec | 6.71 lb/sec |

The mid-frame and aft-frame vent flows and the turbine cooling flow amount to 3.0 and 1.4 percent, respectively, of the inlet airflow:

$$w_{a,mv} + w_{a,av} = (0.030)(6.71)$$

$$= 0.20 \text{ lb/sec}$$

$$w_{a,tc} = (0.014)(6.71)$$

$$= 0.09 \text{ lb/sec}$$

The airflow at other engine stations then becomes

$$w_{a,3} = 6.71 - 0.20 - 0.09$$

$$= 6.42 \text{ lb/sec}$$

$$w_{a,5} = 6.71 - 0.20$$

$$= 6.51 \text{ lb/sec}$$

These airflows are independent of the fuel used.

## Compressor Performance

To determine the compressor operating point, the matching between compressor and turbine must be known. This can be done by the use of the turbine- to compressor-inlet temperature ratio.

From figure 5:

$$T_4/T_1 = 4.69$$

and

$$\sqrt{T_4/T_1} = 2.166$$

From figure 6, the compressor efficiency and compressor-pressure-ratio parameters are:

$$\eta_c = 0.706$$

$$\frac{P_2/P_1}{\sqrt{T_4/T_1}} = 3.875$$

and

$$P_2/P_1 = 8.39$$

The compressor temperature ratio can then be calculated by use of the equation:

$$\frac{T_2}{T_1} = 1 + \frac{(P_2/P_1)^{\frac{\gamma-1}{\gamma}} - 1}{\eta_c}$$

and

$$T_2/T_1 = 2.186$$

The compressor-outlet conditions are:

$$P_2 = 742 \text{ lb/sq ft abs}$$

$$T_2 = 968^\circ \text{ R}$$

## Combustor Performance

To determine combustion efficiency, the calculation of the combustion parameter $w_{a,3}T_6$ is necessary:

| | JP-4 fuel | Gaseous hydrogen |
|---|---|---|
| $w_{a,3}T_6$ | $10.7\times10^3$ | $10.7\times10^3$ |

From figure 7,

| | | |
|---|---|---|
| $\eta_b$ | 0.880 | 0.820 |

The engine temperature rise

| | | |
|---|---|---|
| $T_6 - T_1$ | $1217^\circ$ R | $1217^\circ$ R |

From figure 21 or reference 8 the ideal fuel-air ratio may be determined:

| | | |
|---|---|---|
| $(w_f/3600\ w_{a,5})_{id}$ | 0.01705 | 0.00640 |

Dividing by combustion efficiency to obtain actual fuel-air ratio,

| | | |
|---|---|---|
| $w_f/3600\ w_{a,5}$ | 0.01938 | 0.00780 |

and

| | | |
|---|---|---|
| $w_f$ | 454 lb/hr | 183 lb/hr |

To determine the combustor total-pressure loss, the following steps are necessary. Because the small shift in the compressor operating point with change in fuels has been neglected, the turbine-inlet pressure and temperature for both fuels will be identical:

$$T_4 = (4.69)(442.6)$$

$$= 2076^{\circ} \text{ R}$$

The combustor temperature ratio is

$$T_4/T_2 = 2.145$$

From figure 8,

$$(P_2 - P_4)/P_2 = 0.0470$$

and

$$P_4 = 707 \text{ lb/sq ft abs}$$

Turbine Performance

In order to determine turbine performance the corrected turbine speed must be calculated:

$$\sqrt{\theta_4} = 2.000$$

$$N/\sqrt{\theta_4} = 3050 \text{ rpm}$$

The turbine Reynolds number index can then be determined from figure 10:

$$\delta_4/\varphi_4\sqrt{\theta_4} = 0.066$$

From figure 9, the corrected turbine gas flow and turbine efficiency can be determined:

$$w_{g,4}\sqrt{\theta_4}\beta_4/\delta_4 = 40.5 \text{ lb/sec}$$

$$\eta_t = 0.720$$

These values are valid regardless of which fuel is used. The turbine total-pressure ratio is

| | JP-4 fuel | Gaseous hydrogen |
|---|---|---|
| $P_4/P_5$ = | 707/188 | 707/196 |
| = | 3.76 | 3.61 |

From figure 9, the corrected turbine work is

| | JP-4 fuel | Gaseous hydrogen |
|---|---|---|
| $\Delta H/\theta_4$ | = 28.5 Btu/lb | 28.5 Btu/lb |

Exhaust-System Performance

To obtain the exhaust-nozzle total pressure, it is necessary to determine the tailpipe-pressure loss. To do this, the following steps are necessary:

| | JP-4 fuel | Gaseous hydrogen |
|---|---|---|
| $w_{g,5}$ | = 6.51 + 454/3600 | 6.51 + 183/3600 |
| | = 6.64 lb/sec | 6.56 lb/sec |
| $T_9 = T_6$ | = 1660° R | 1660° R |
| $w_{g,5}\sqrt{T_9}/P_5$ | = 1.439 | 1.364 |

From figure 11,

| | | |
|---|---|---|
| $(P_5 - P_9)/P_5$ | = 0.037 | 0.028 |

and

| | | |
|---|---|---|
| $P_9$ | = 181 lb/sq ft abs | 191 lb/sq ft abs |

The exhaust-nozzle pressure ratio is

| | | |
|---|---|---|
| $P_9/p_0$ | = 3.12 | 3.29 |

From figure 11, the exhaust-nozzle velocity coefficient is

| | | |
|---|---|---|
| $C_v$ | = 0.985 | 0.985 |

Over-All Engine Performance

To calculate thrust, the effective velocity must be determined. To do this the following steps are neceessary:

From figure 22, the ratio of specific heats at the exhaust nozzle is

| | JP-4 fuel | Gaseous hydrogen |
|---|---|---|
| $\gamma_9$ = | 1.327 | 1.333 |

From figure 23 or reference 6, the effective velocity parameter can be found:

| | | |
|---|---|---|
| $V_{eff}/\sqrt{gRT_6}$ = | 1.396 | 1.420 |

The gas constant of the exhaust products when using JP-4 fuel is very nearly a constant and is normally considered to be 53.4 ft-lb/(lb)($^{\circ}$R). When using gaseous-hydrogen fuel the gas constant of the exhaust products varies with the amount of fuel added (see fig. 24):

| | | |
|---|---|---|
| R = | 53.4 ft-lb(lb)($^{\circ}$R) | 55.9 ft-lb/(lb)($^{\circ}$R) |

and

| | | |
|---|---|---|
| $\sqrt{gRT_6}$ = | 1689 ft/sec | 1728 ft/sec |

The effective velocity then becomes

| | | |
|---|---|---|
| $V_{eff}$ = | 2358 ft/sec | 2454 ft/sec |

and the jet thrust is

| | | |
|---|---|---|
| $F_j$ = | $\frac{w_{g,5}}{g} C_v V_{eff}$ | $\frac{w_{g,5}}{g} C_v V_{eff}$ |
| = | 479 lb | 493 lb |

Subtracting the inlet momentum, the net thrust becomes

| | | |
|---|---|---|
| $F_n = F_j - \frac{w_{a,1}}{g} V_0$ | | $F_j - \frac{w_{a,1}}{g} V_0$ |
| = | 317 lb | 331 lb |

and the specific fuel consumption is

| | | |
|---|---|---|
| $w_f/F_n$ = | 1.432 lb/(hr) (lb thrust) | 0.553 lb/(hr) (lb thrust) |

Since the exhaust nozzle is choked, the effective exhaust-nozzle area can be determined from the total-pressure parameter of figure 25. If the exhaust nozzle is not choked, the total-pressure parameter can be obtained from reference 5.

| | JP-4 fuel | Gaseous hydrogen |
|---|---|---|
| $\frac{P_9 A_{10,eff}}{w_{g,9}\sqrt{T_9 R/g}}$ | 1.485 | 1.483 |
| $A_{10,e}$ | 2.86 sq ft | 2.74 sq ft |

## REFERENCES

1. Silverstein, Abe, and Hall, Eldon W.: Liquid Hydrogen as a Jet Fuel for High-Altitude Aircraft. NACA RM E55C28a, 1955.

2. Fleming, W. A., Kaufman, H. R., Harp, J. L., Jr., and Chelko, L. J.: Turbojet Performance and Operation at High Altitudes with Hydrogen and JP-4 Fuels. NACA RM E56E14, 1956.

3. Glawe, George E., Simmons, Frederick S., and Stickney, Truman M.: Radiation and Recovery Corrections and Time Constants of Several Chromel-Alumel Thermocouple Probes in High-Temperature, High-Velocity Gas Streams. NACA TN 3766, 1956.

4. Prince, William R., and Wile, Darwin B.: Altitude Performance of Compressor, Turbine, and Combustor Components of X600-B9 Turbojet Engine. NACA RM E53I18, 1954.

5. Sivo, Joseph N., and Fenn, David B.: Performance of a Short Combustor at High Altitudes Using Hydrogen Fuel. NACA RM E56D24, 1956.

6. Turner, L. Richard, Addie, Albert N., and Zimmerman, Richard H.: Charts for the Analysis of One-Dimensional Steady Compressible Flow. NACA TN 1419, 1948.

7. English, Robert E., and Wachtl, William W.: Charts of Thermodynamic Properties of Air and Combustion Products from 300° to 3500° R. NACA TN 2071, 1950.

8. Turner, L. Richard, and Bogart, Donald: Constant-Pressure Combustion Charts Including Effects of Diluent Addition. NACA Rep. 937, 1949. (Supersedes NACA TN's 1086 and 1655.)

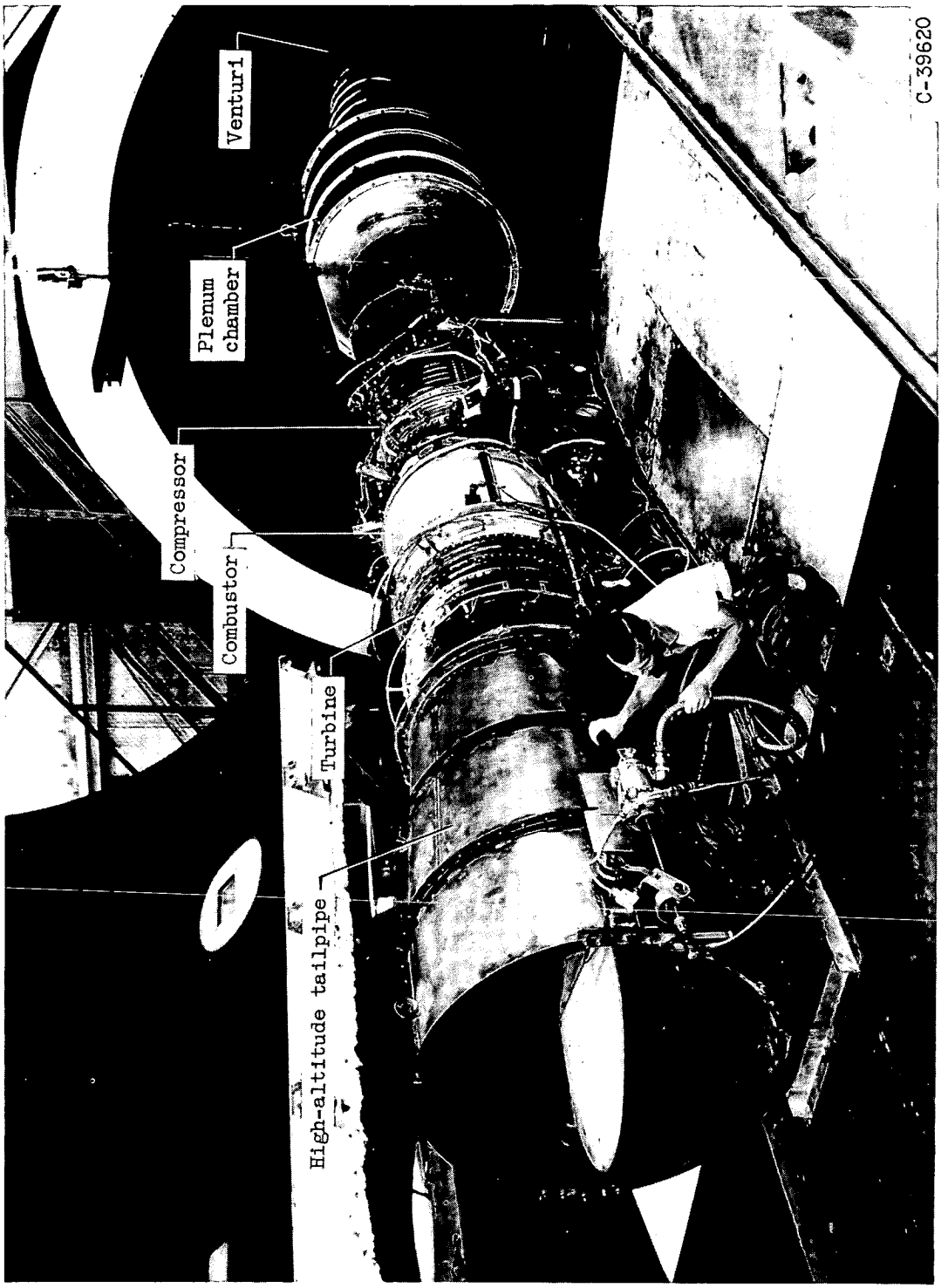


Figure 1. - Installation of J71-A-11 turbojet engine in altitude wind tunnel.

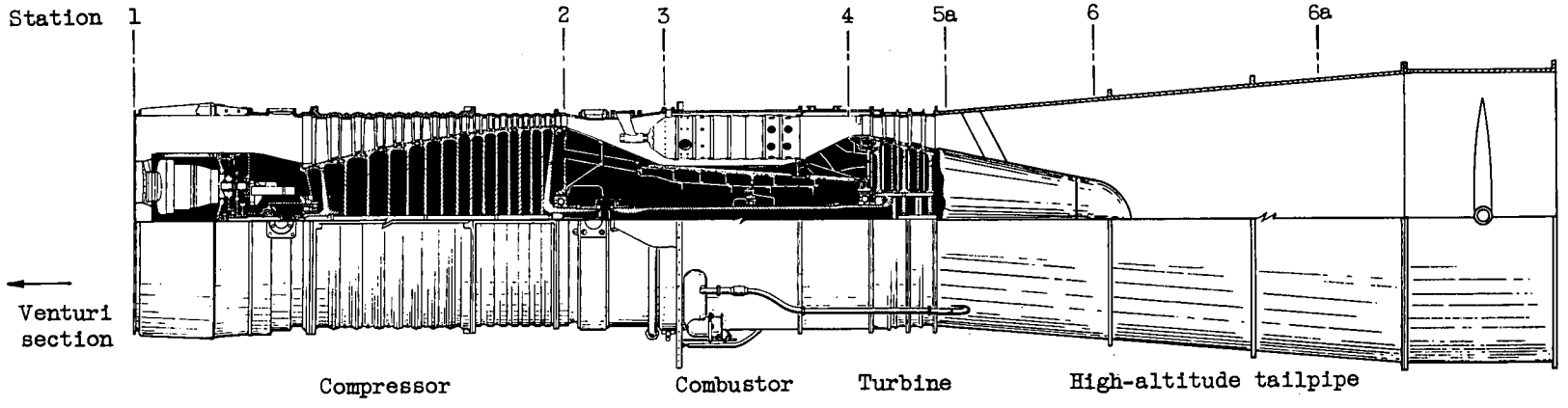


| Station | Total-pressure probes | Stream static pressure | Temperature probes |
|---|---|---|---|
| Venturi | 18 | 5 | 4 |
| 1 | 36 | 16 | 16 |
| 2 | 20 | - | 16 |
| 3 | - | - | - |
| 4 | 20 | - | 10 |
| 5 | 15 | - | 15 |
| 5a | 32 | - | 16 |
| 6 | 24 | - | - |
| 6a | - | - | 7 |
| 9 | 20 | - | 16 |

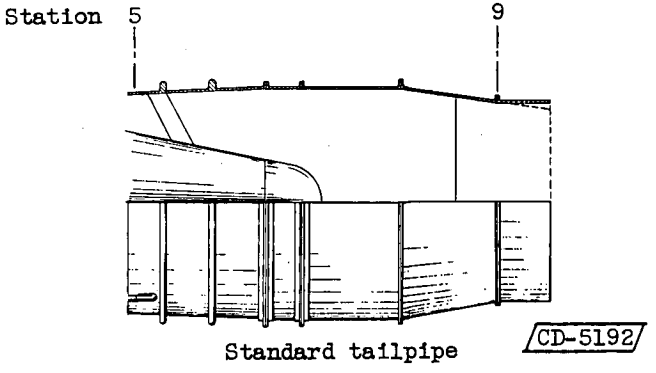


Figure 2. - Location of instrumentation within J71-A-11 turbojet engine for exhaust diffuser and standard tailpipe installations.

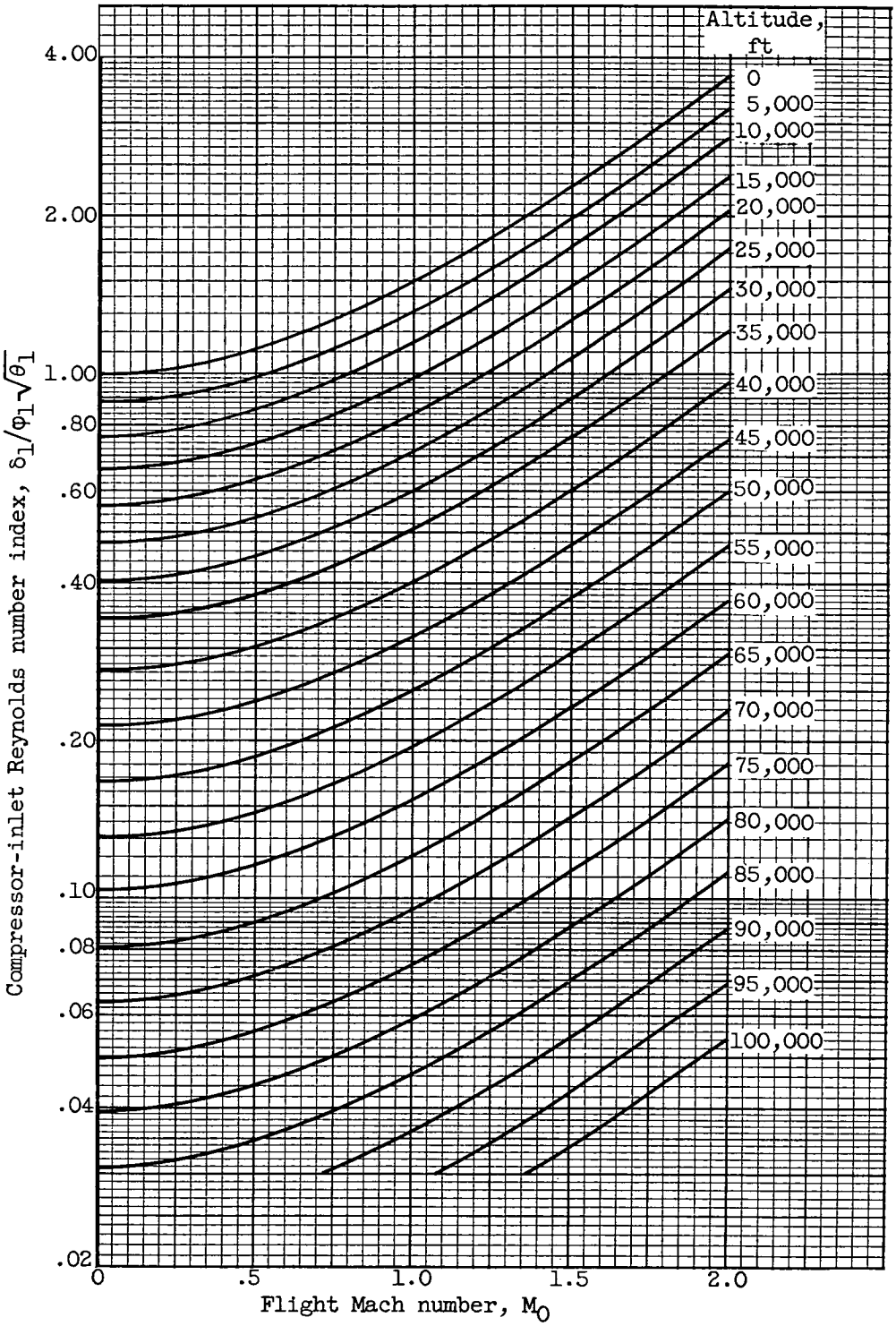


Figure 3. - Reynolds number indices for a range of altitudes and flight Mach numbers for NACA standard atmosphere and 100-percent ram-pressure recovery.

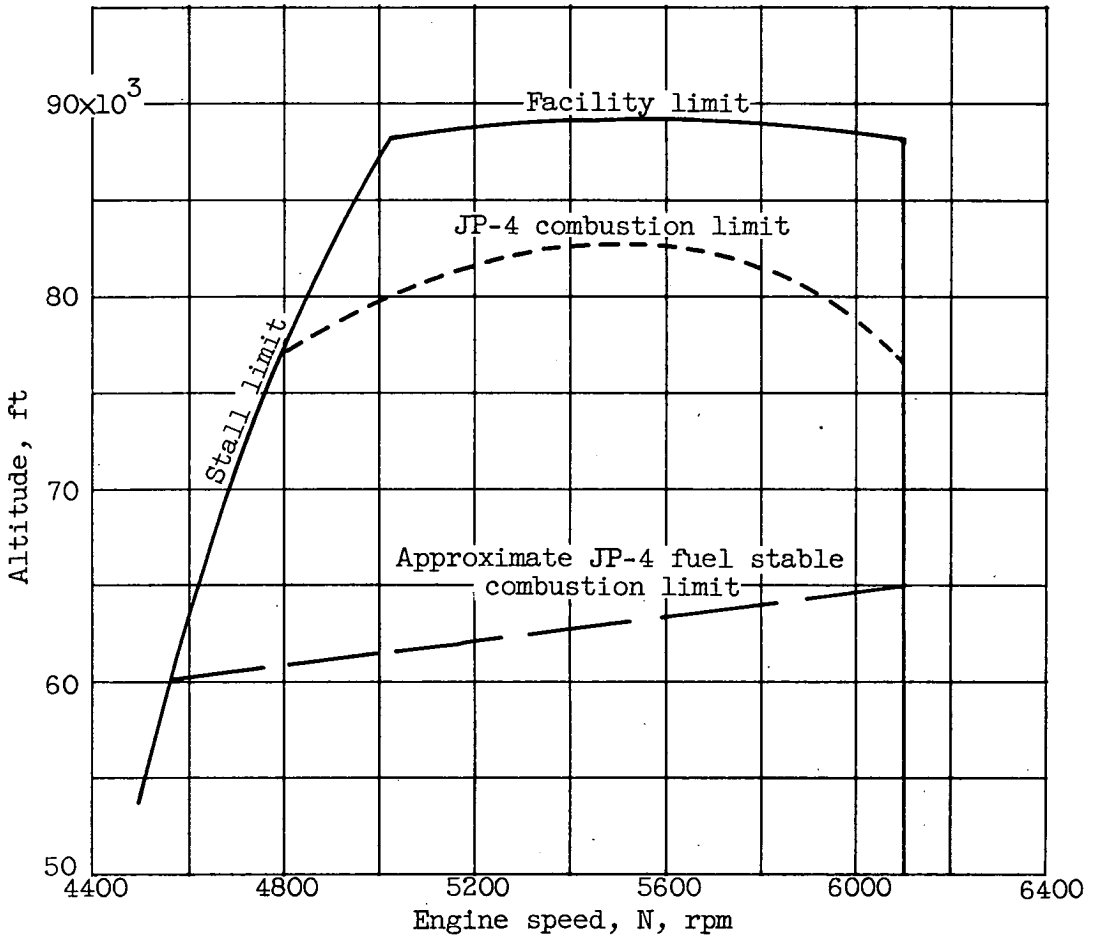


Figure 4. - Operating limits at flight Mach number of 0.8 and NACA standard altitude conditions.

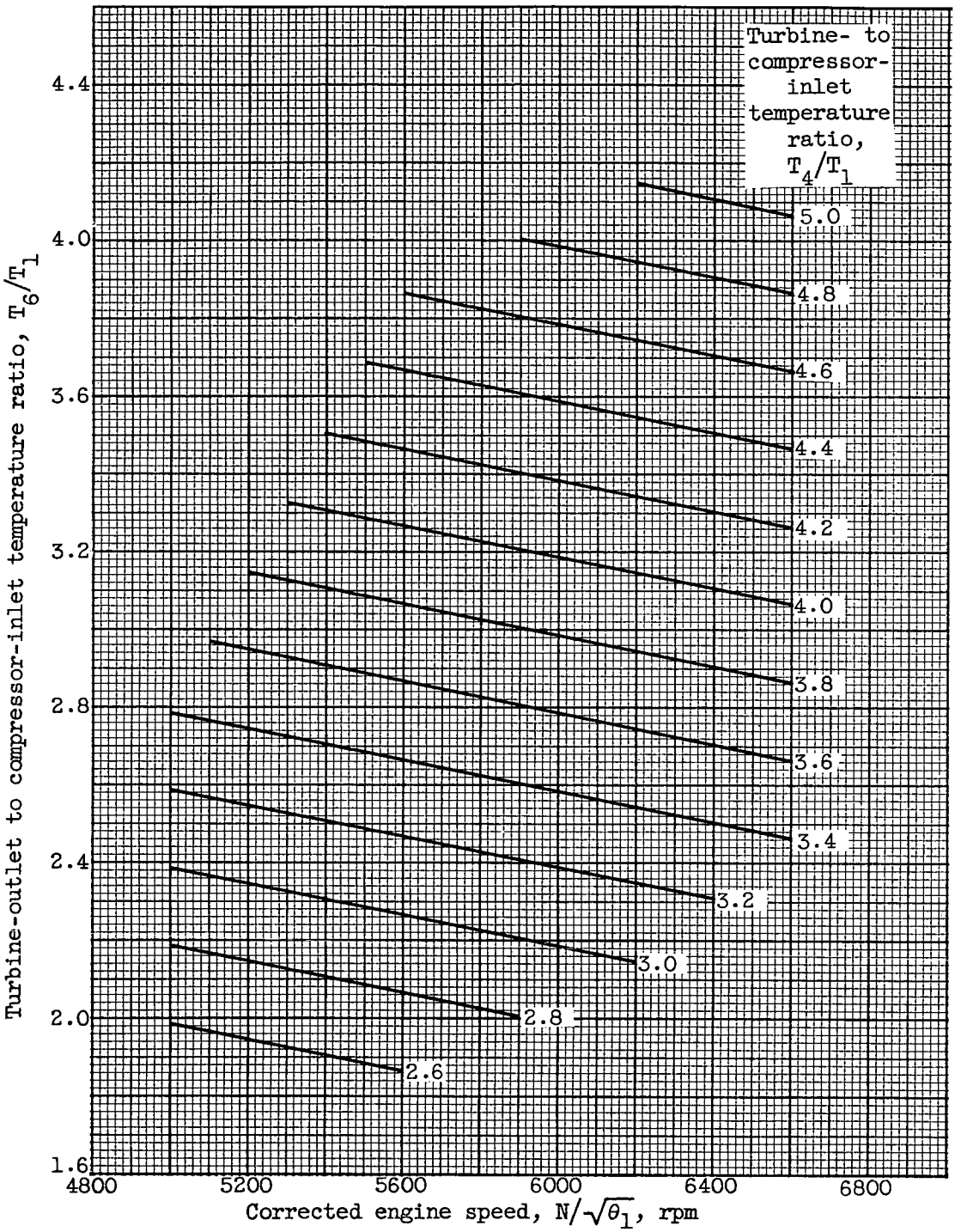


Figure 5. - Relationship between turbine-inlet and -outlet temperature. Valid for JP-4 and gaseous-hydrogen fuels at all compressor-inlet Reynolds number indices within the range investigated.

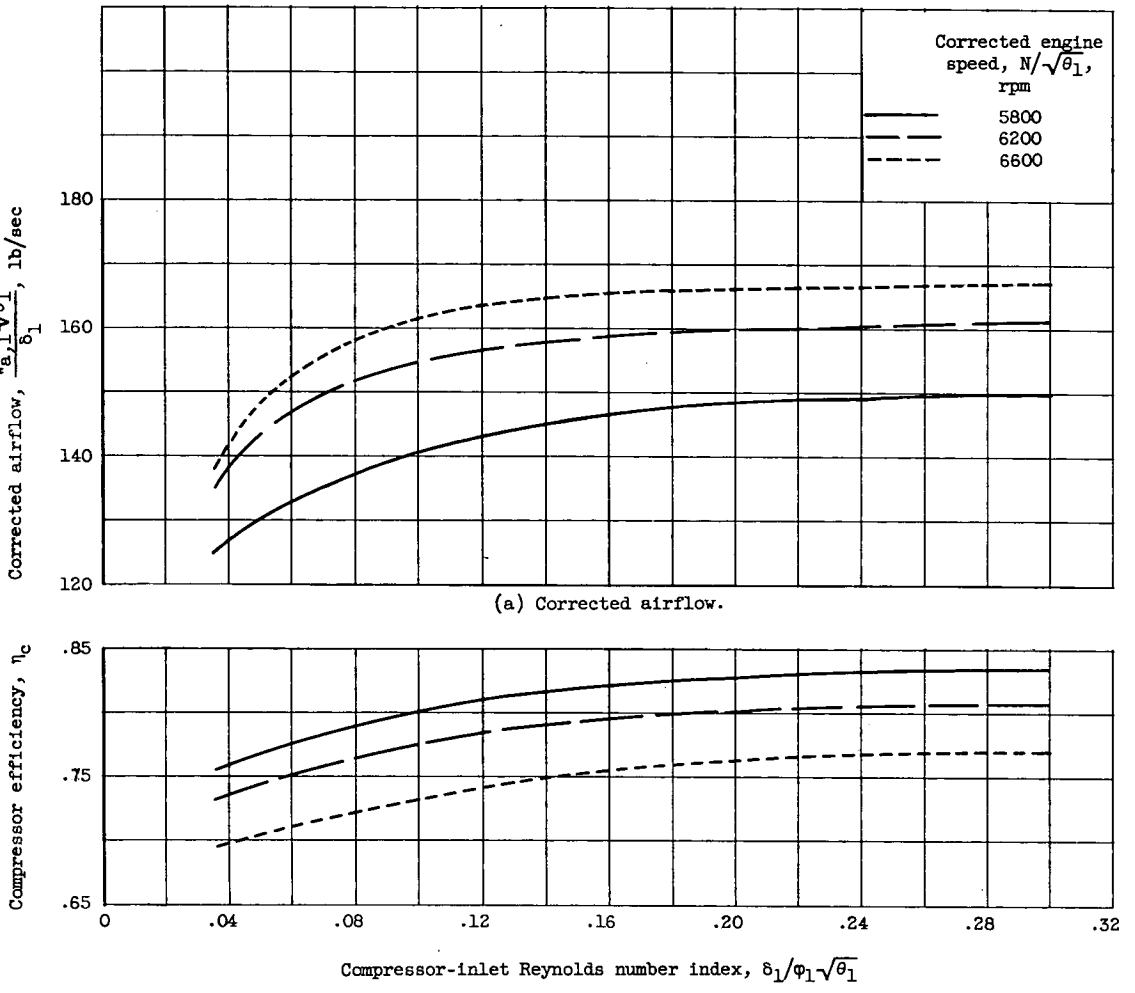


(a) Corrected airflow.

(b) Compressor efficiency.

Figure 6. - Compressor performance for range of compressor-inlet Reynolds number index.

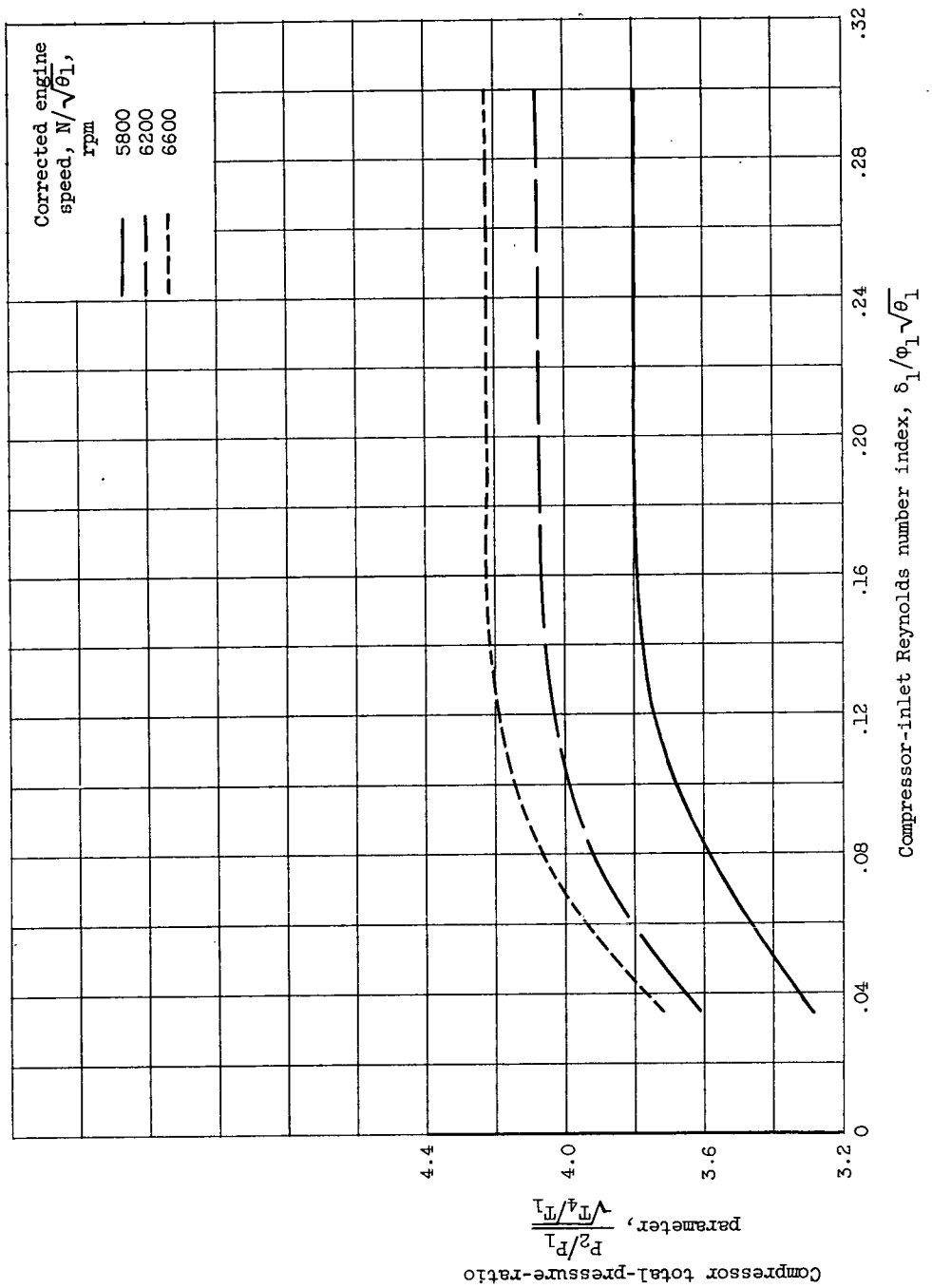


(c) Compressor total-pressure-ratio parameter.

Figure 6. - Continued. Compressor performance for range of compressor-inlet Reynolds number index.

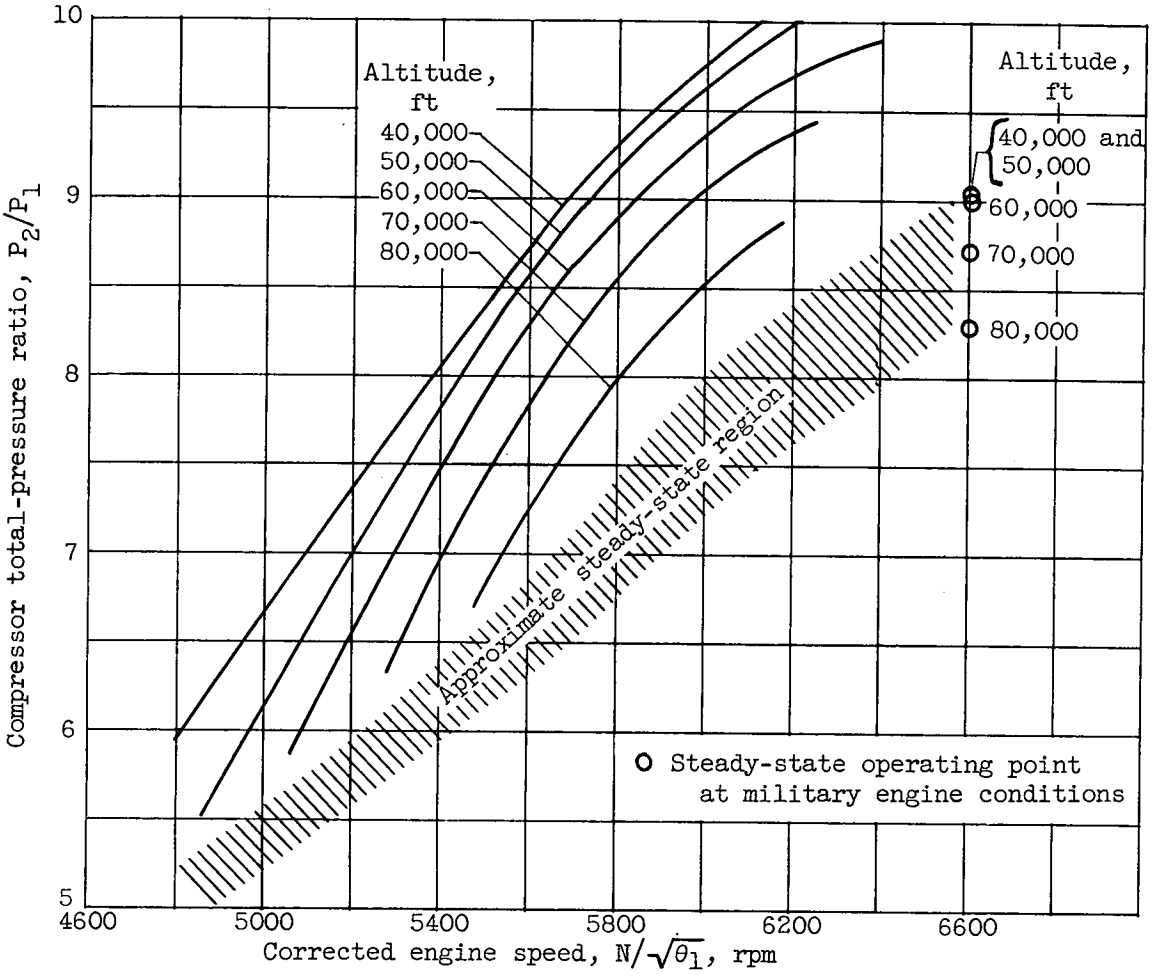


(d) Stall limit at flight Mach number of 0.8.

Figure 6. - Concluded. Compressor performance for range of compressor-inlet Reynolds number index.

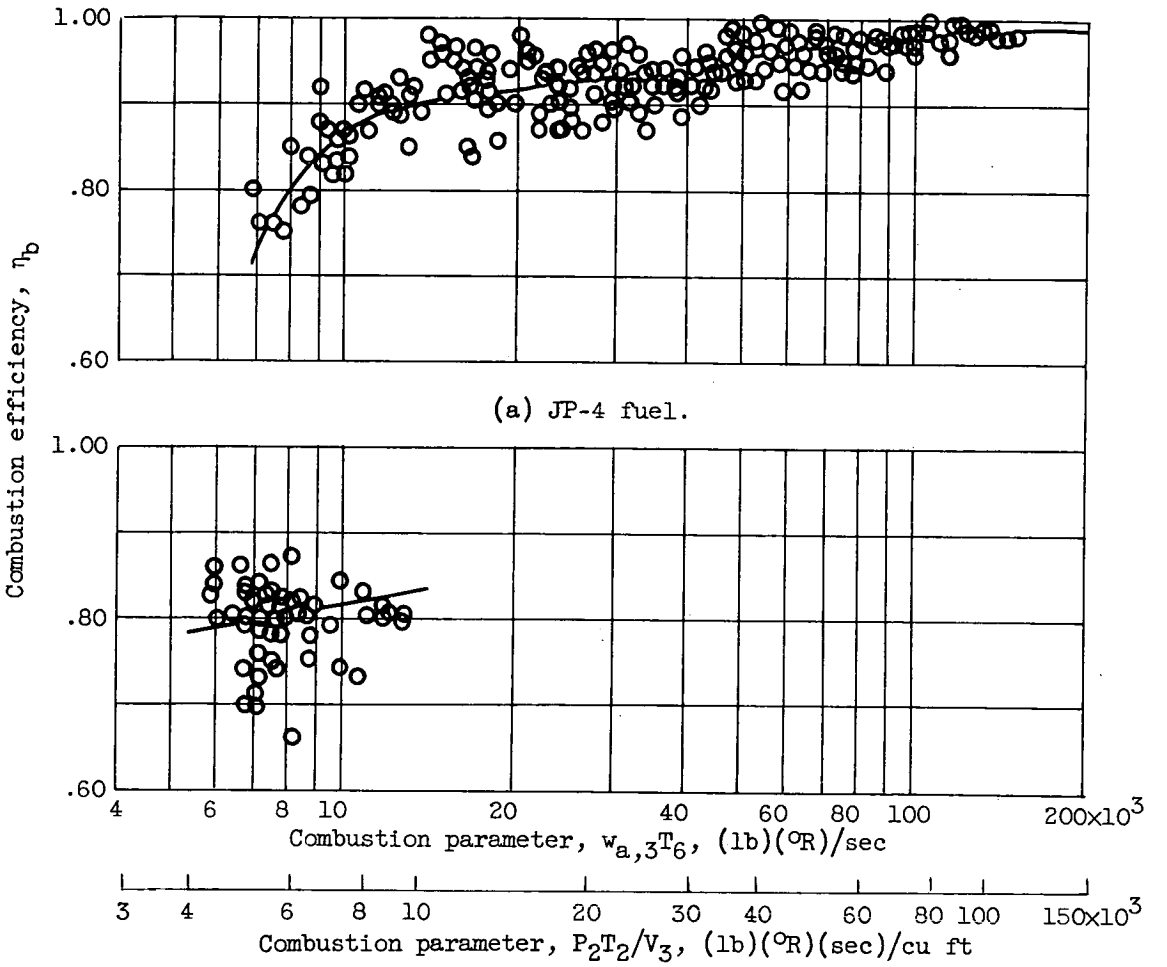


(b) Gaseous-hydrogen fuel.

Figure 7. - Combustion efficiency.

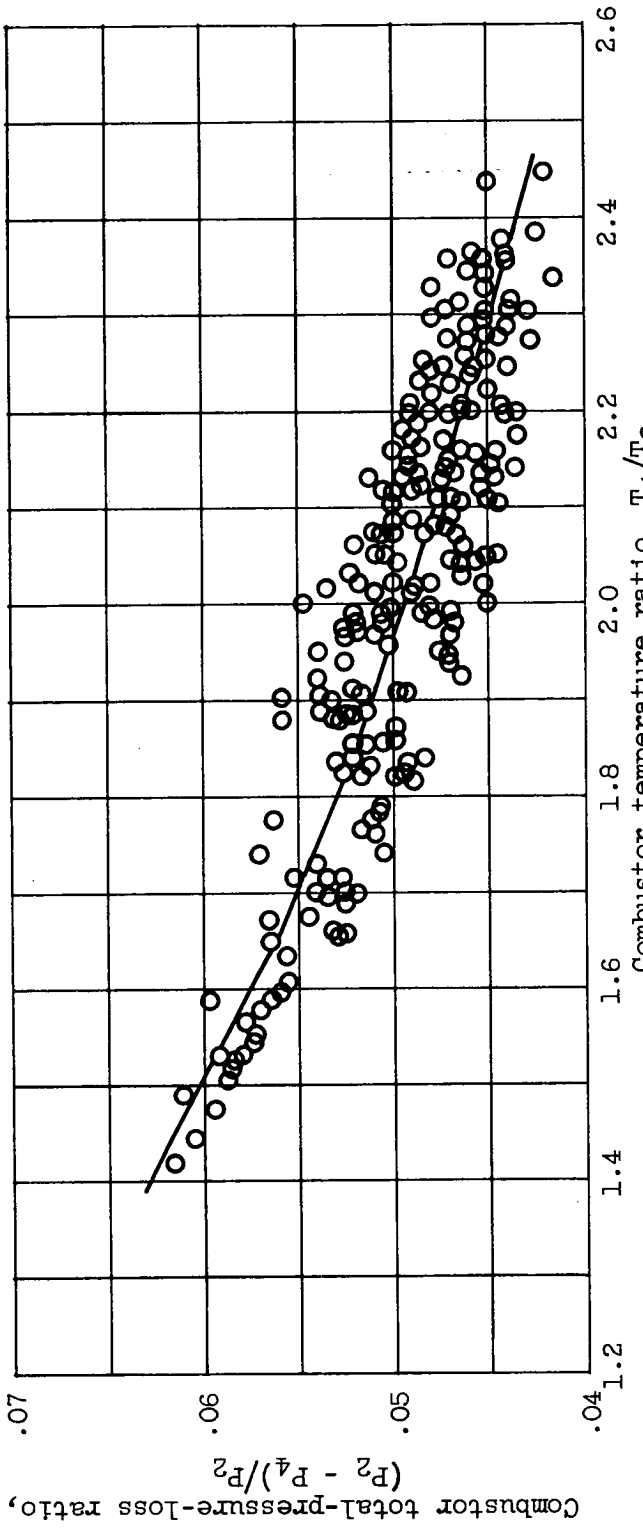


Figure 8. - Combustor total-pressure loss.

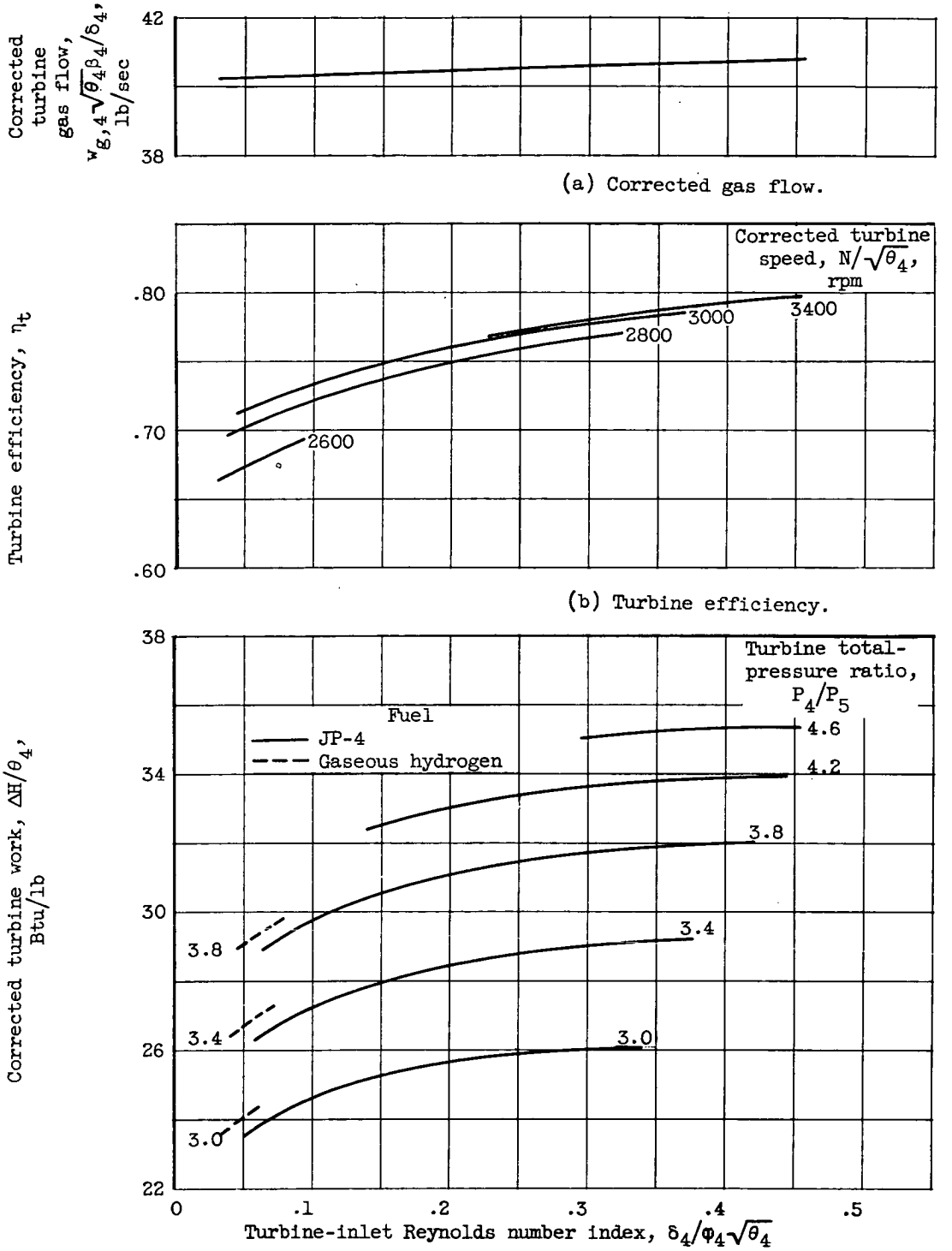


Figure 9. - Turbine performance for range of Reynolds number index.

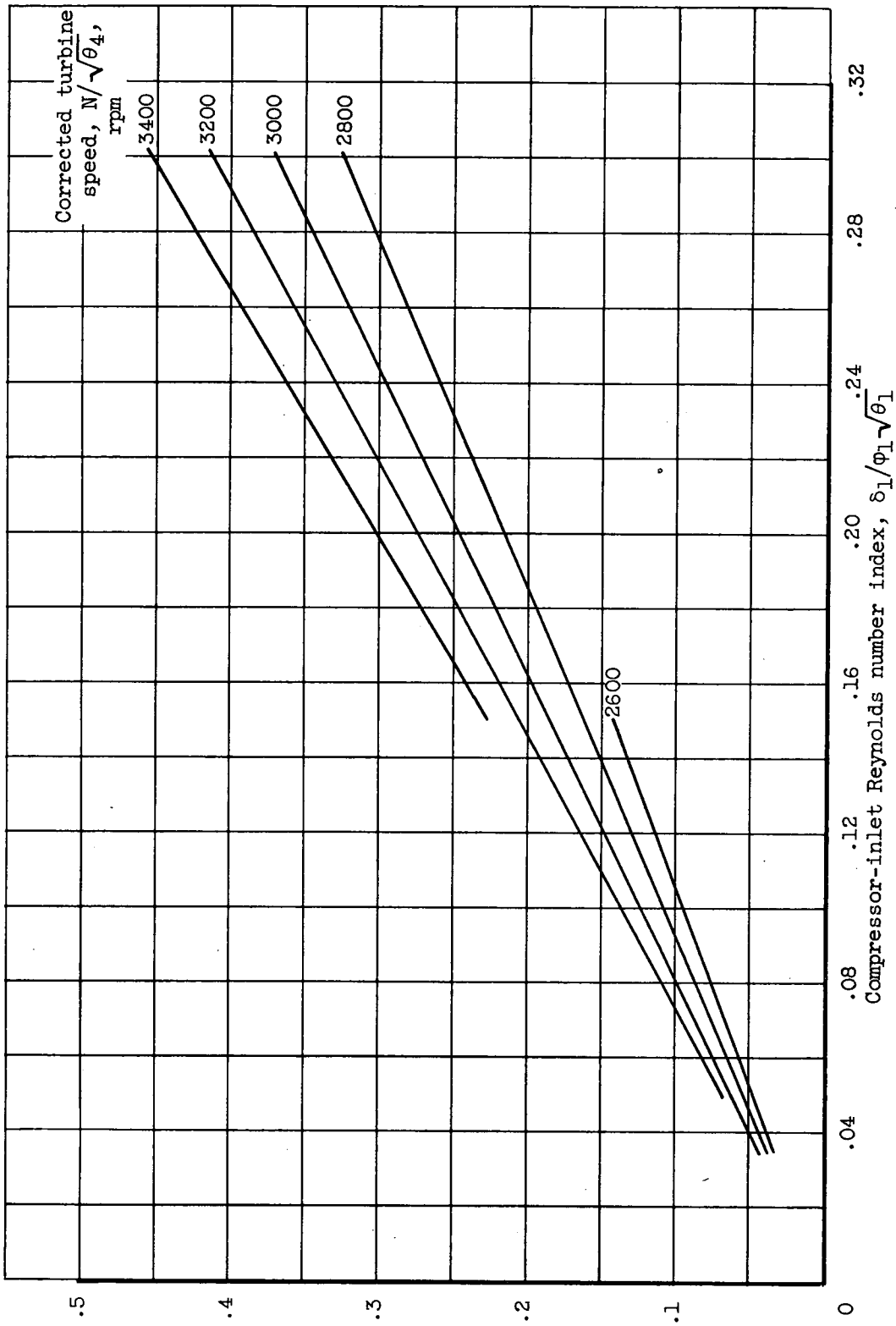


Figure 10. - Approximate relation between turbine- and compressor-inlet conditions.

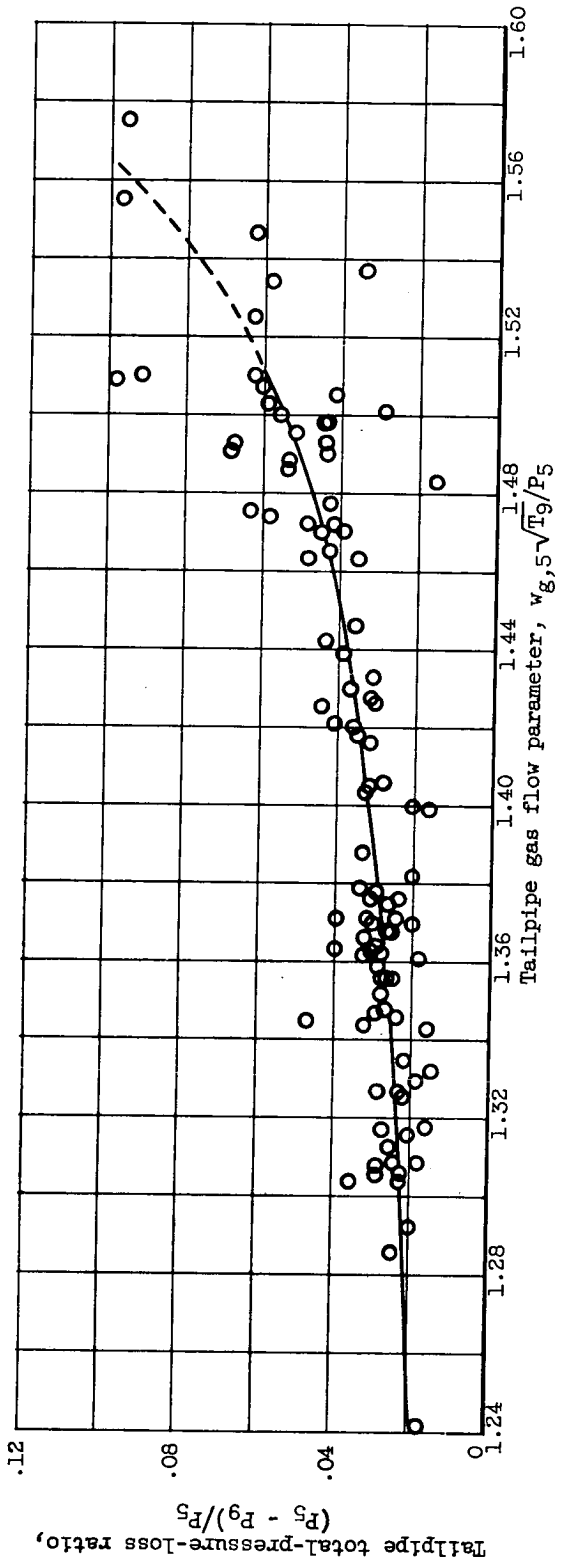


(a) Tailpipe total-pressure loss.

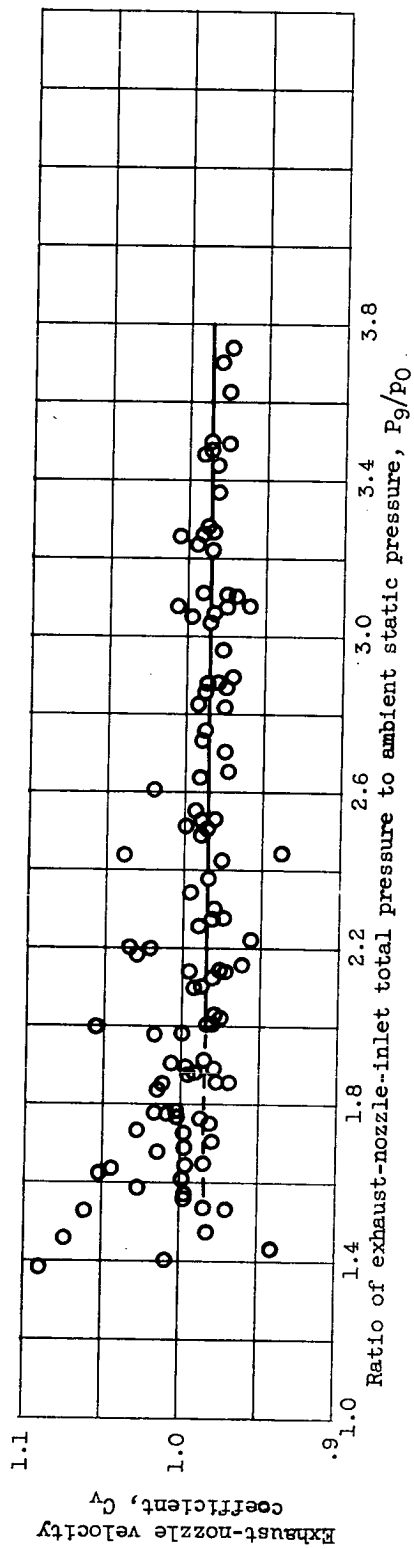


(b) Exhaust-nozzle velocity coefficient.

Figure 11. - Exhaust-system losses.

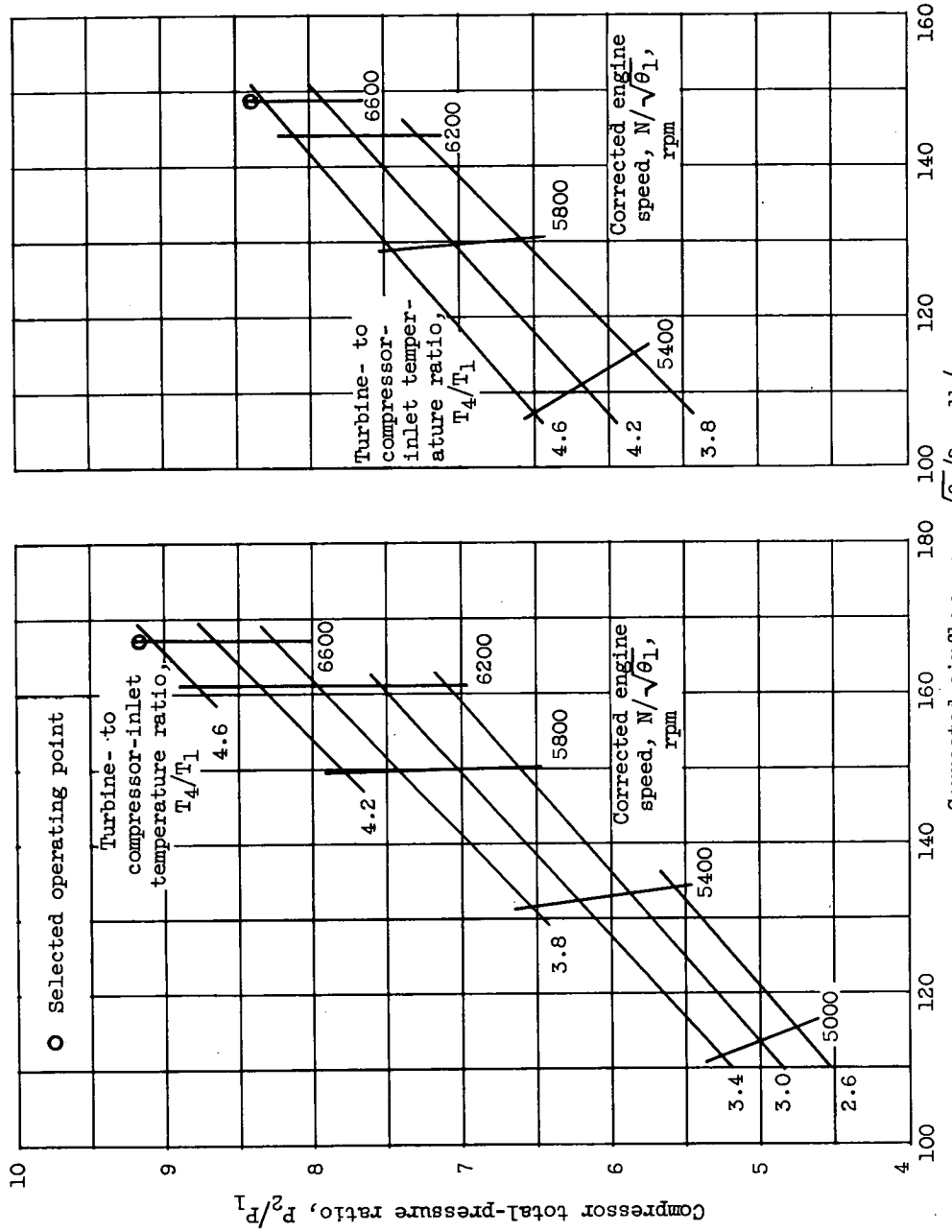


(a) Compressor-inlet Reynolds number index, 0.30.

(b) Compressor-inlet Reynolds number index, 0.05.

Figure 12. - Compressor performance maps.

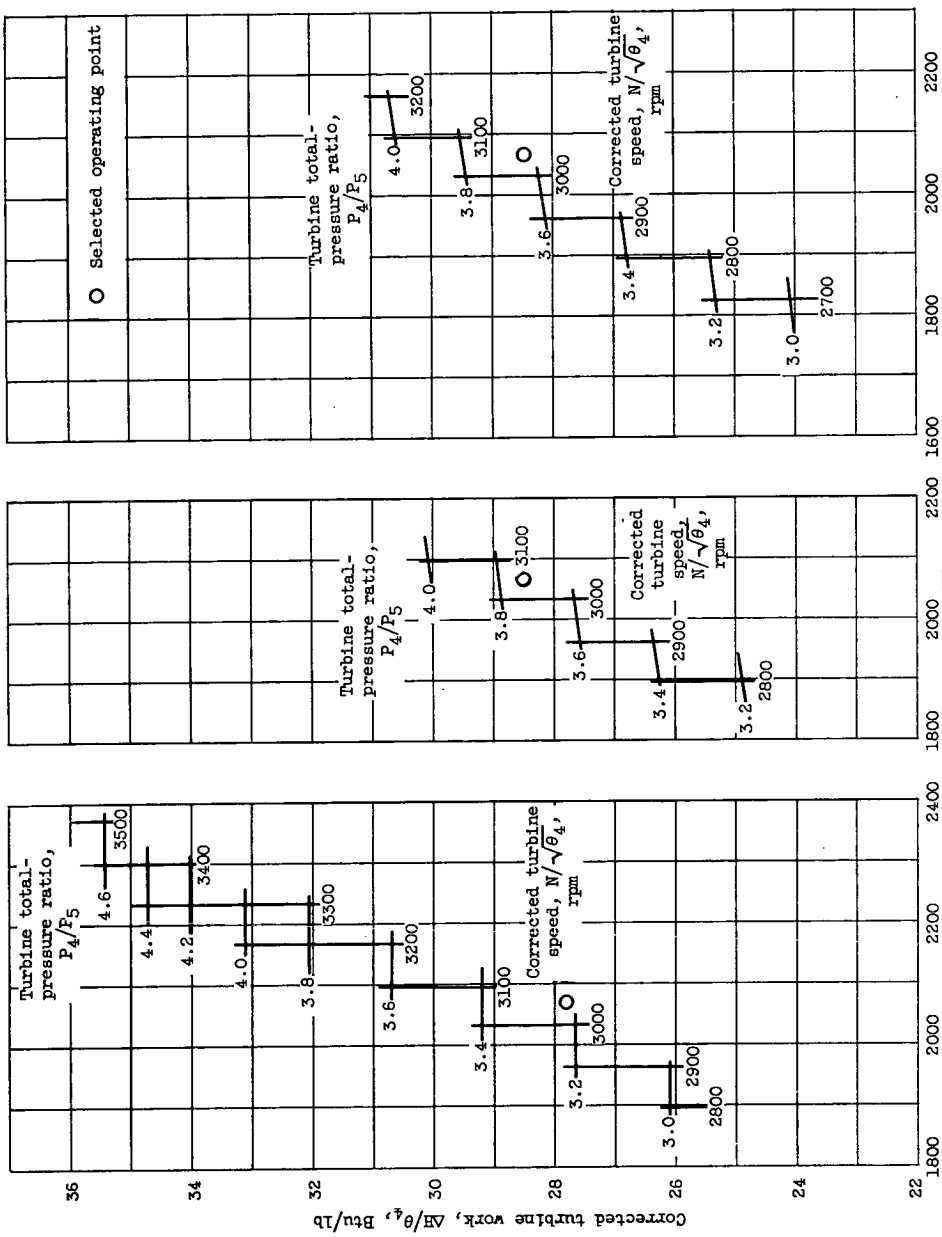


(a) Compressor-inlet Reynolds number index, 0.30; fuel, JP-4.

(b) Compressor-inlet Reynolds number index, 0.05; fuel, JP-4.

(c) Compressor-inlet Reynolds number index, 0.05; fuel, gaseous hydrogen.

Figure 13. - Turbine performance maps.

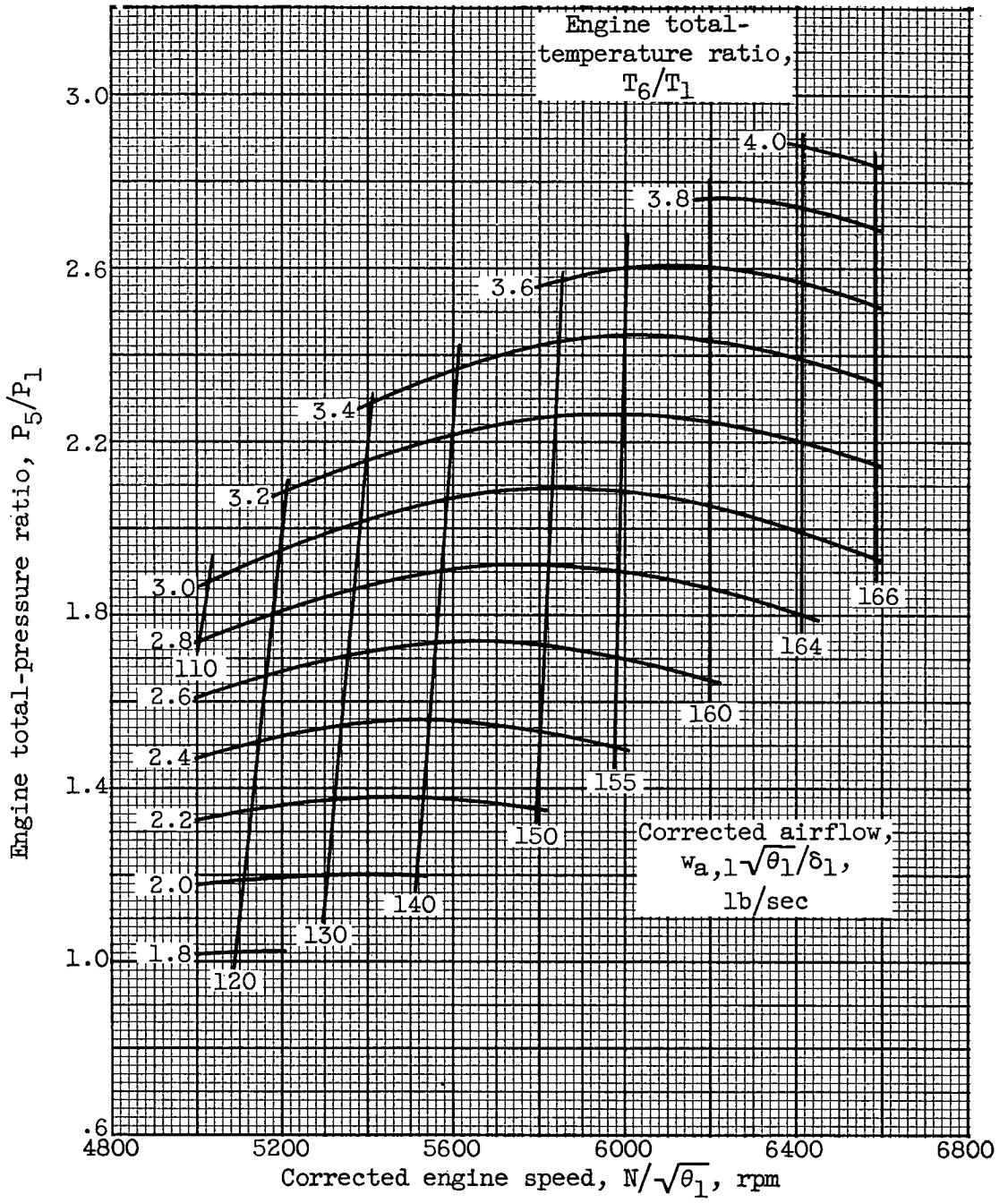


(a) Pumping map at Reynolds number index of 0.20.

Figure 14. - Engine pumping characteristics using JP-4 fuel.

(b) Pumping characteristic corrections for Reynolds number indices other than 0.20 at constant engine total-temperature ratio and corrected engine speed.

Figure 14. - Concluded. Engine pumping characteristics using JP-4 fuel.

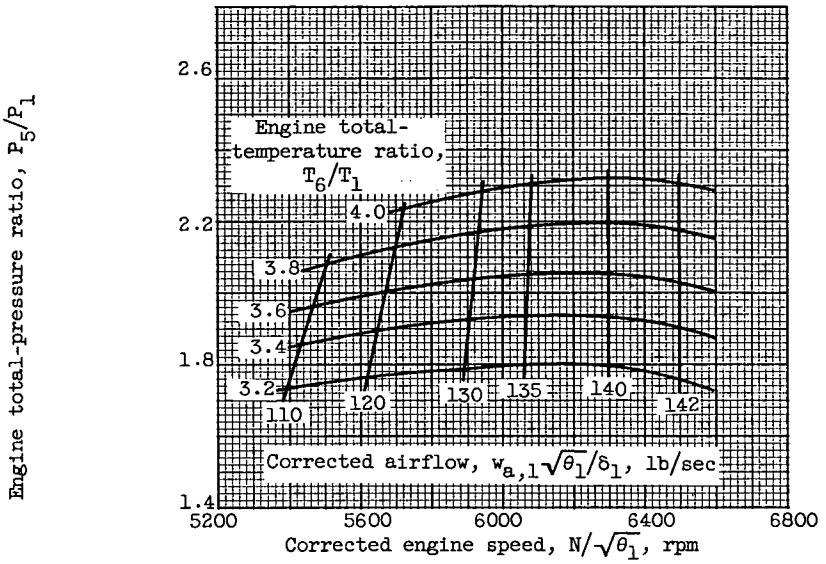


(a) Pumping map at Reynolds number index of 0.04.

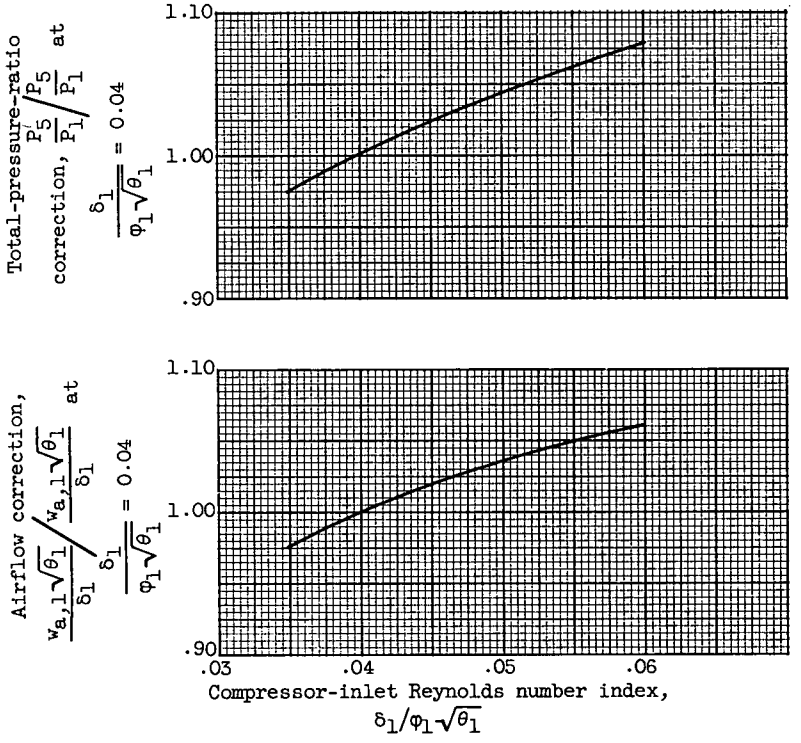


(b) Pumping characteristic corrections for Reynolds number indices other than 0.04 at constant engine total-temperature ratio and corrected engine speed.

Figure 15. - Engine pumping characteristics using gaseous-hydrogen fuel.

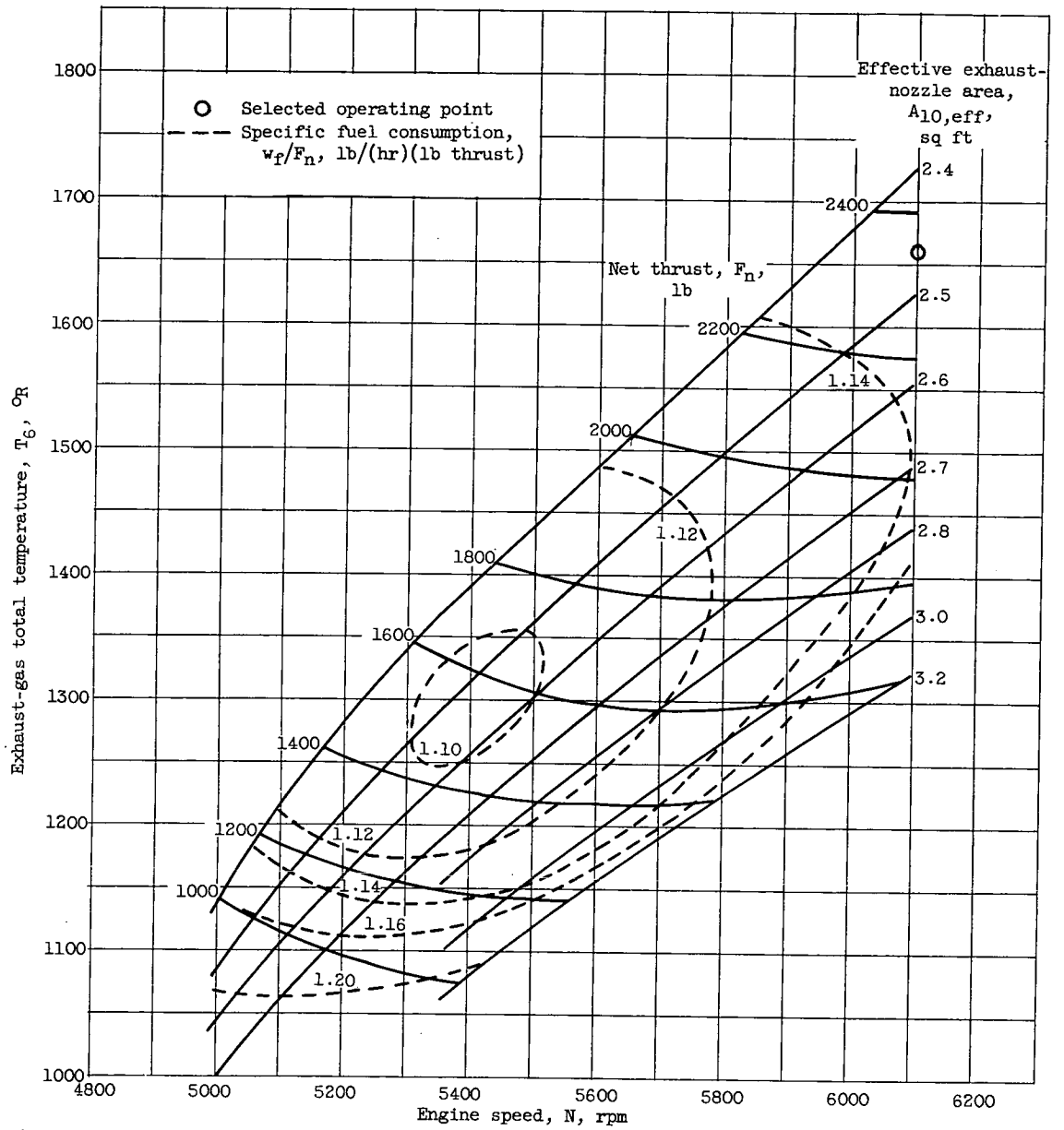


(a) Altitude, 43,000 feet; compressor-inlet Reynolds number index, 0.30; fuel, JP-4.

Figure 16. - Engine performance maps at flight Mach number of 0.80.

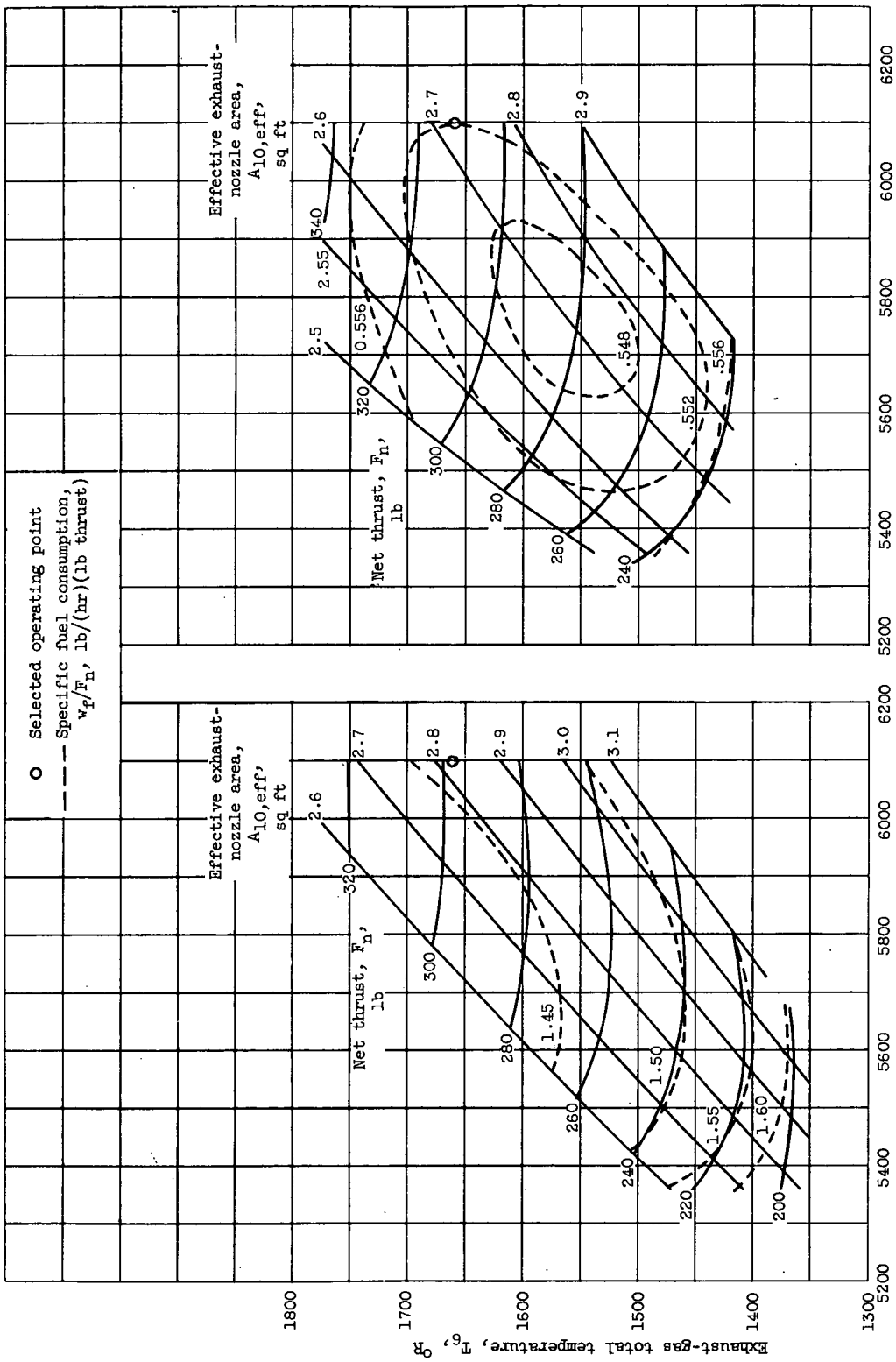


(b) Altitude, 81,000 feet; compressor-inlet Reynolds number index, 0.05; fuel, JP-4.

(c) Altitude, 81,000 feet; compressor-inlet Reynolds number index, 0.05; fuel, gaseous hydrogen.

Figure 16. - Concluded. Engine performance maps at flight Mach number of 0.80.

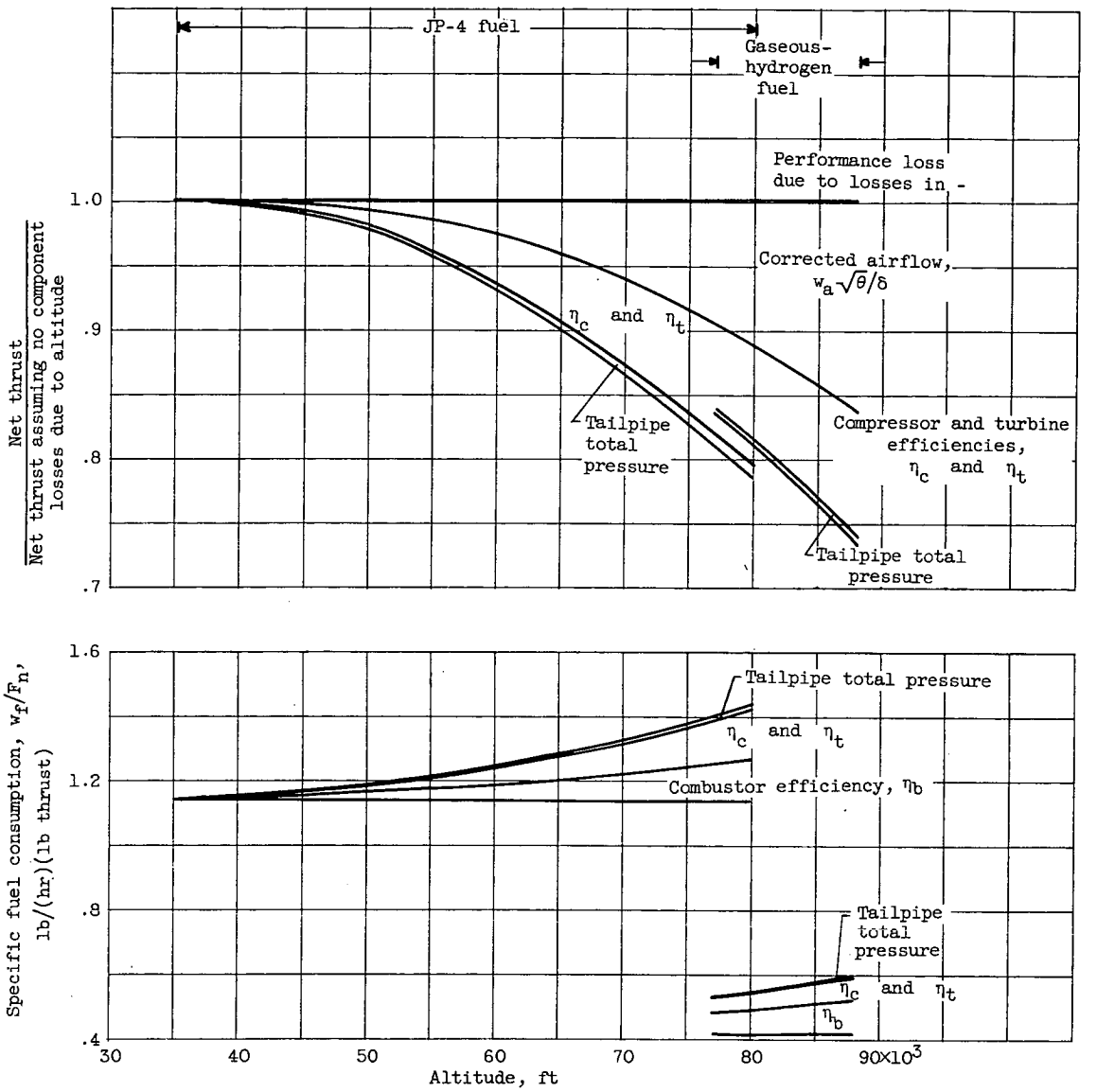


Figure 17. - Effect of individual component performance on over-all engine performance over range of altitude. Flight Mach number, 0.8; engine speed, 6100 rpm; exhaust-gas total temperature, 1200° F.

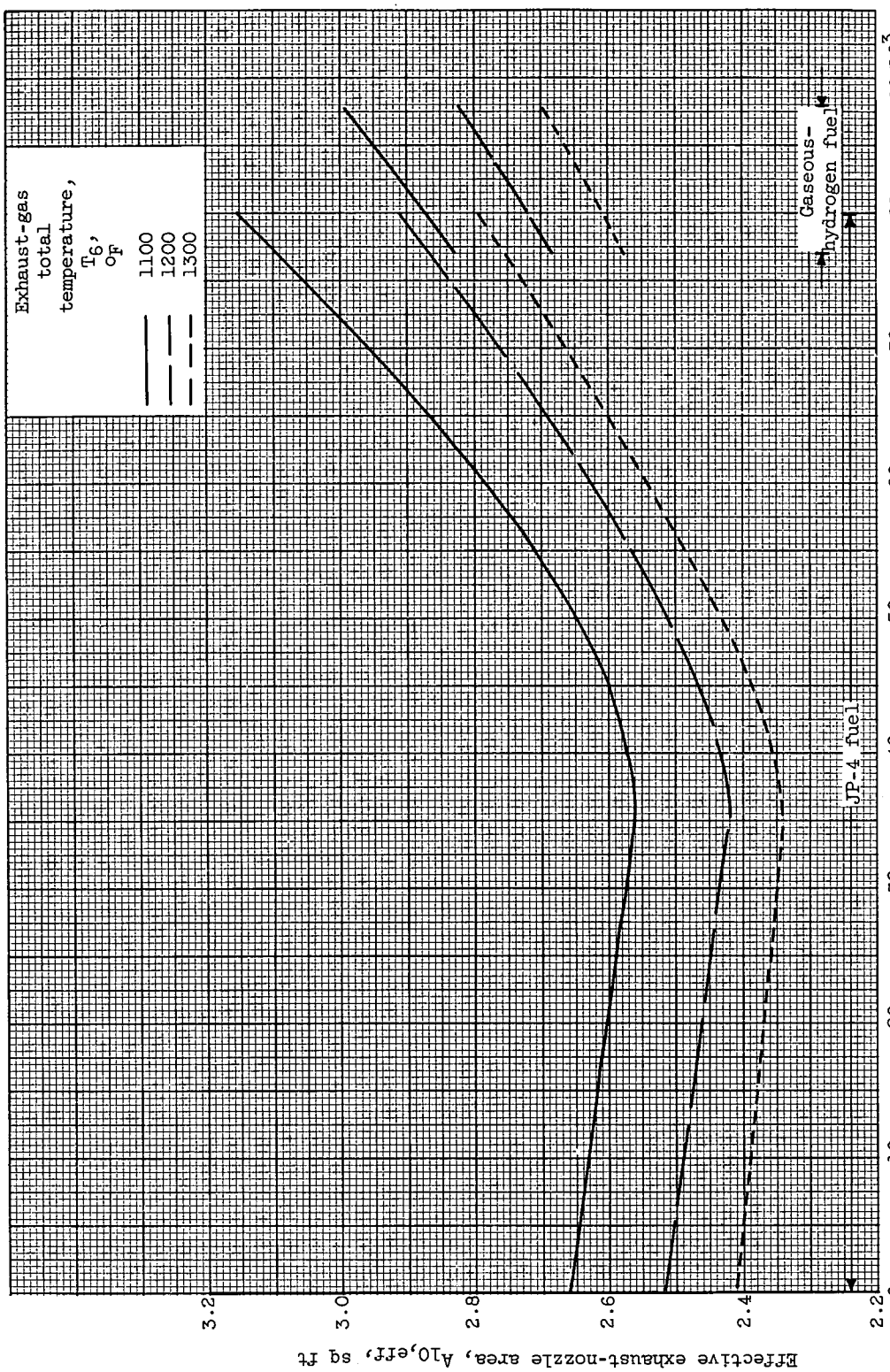


Figure 18. - Effective exhaust-nozzle area required to maintain three constant exhaust-gas total temperatures over range of altitude. Flight Mach number, 0.8; engine speed, 6100 rpm.

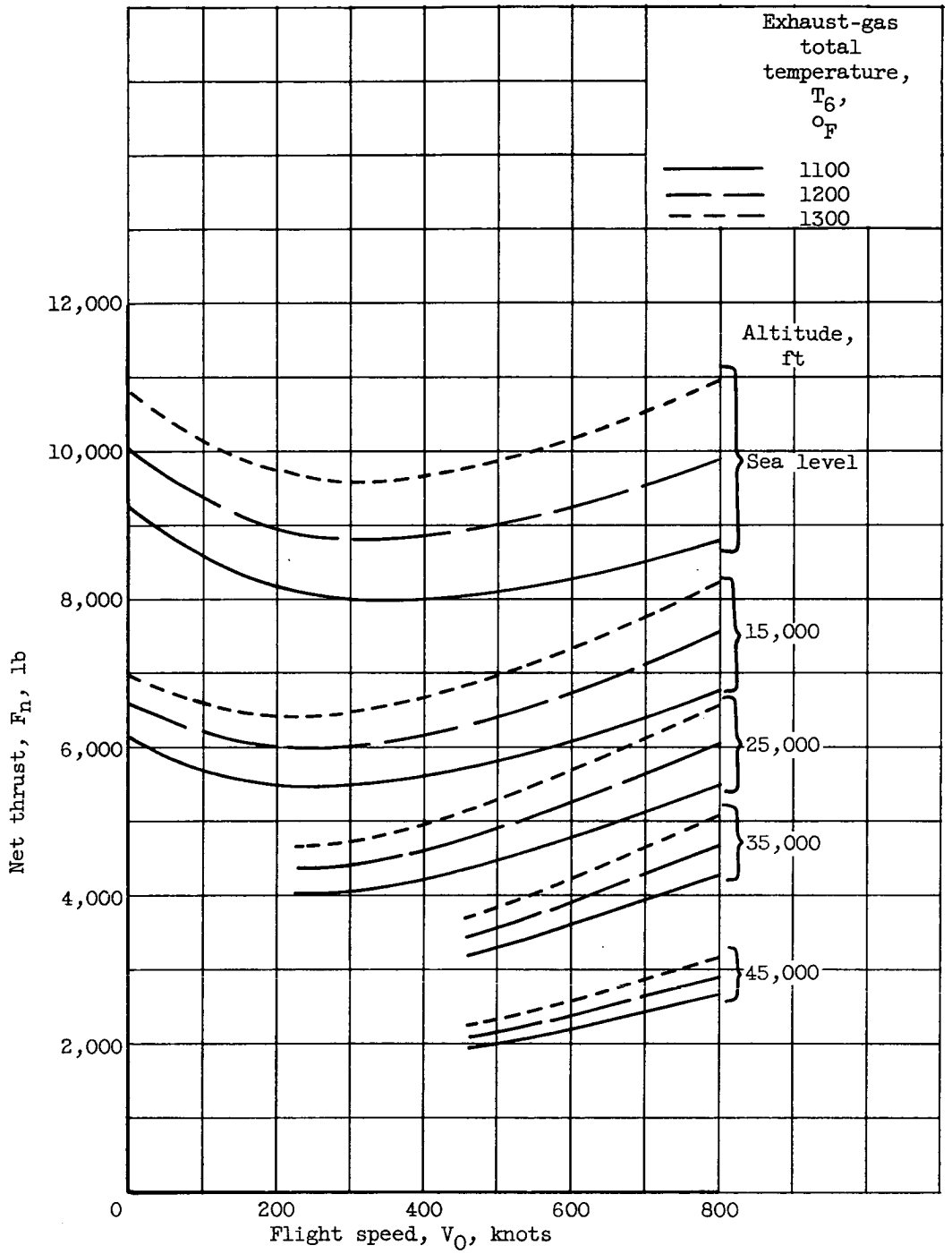


(a) Net thrust.

Figure 19. - Low-altitude performance using JP-4 fuel. Engine speed, 6100 rpm; NACA standard atmosphere; 100-percent ram-pressure recovery.

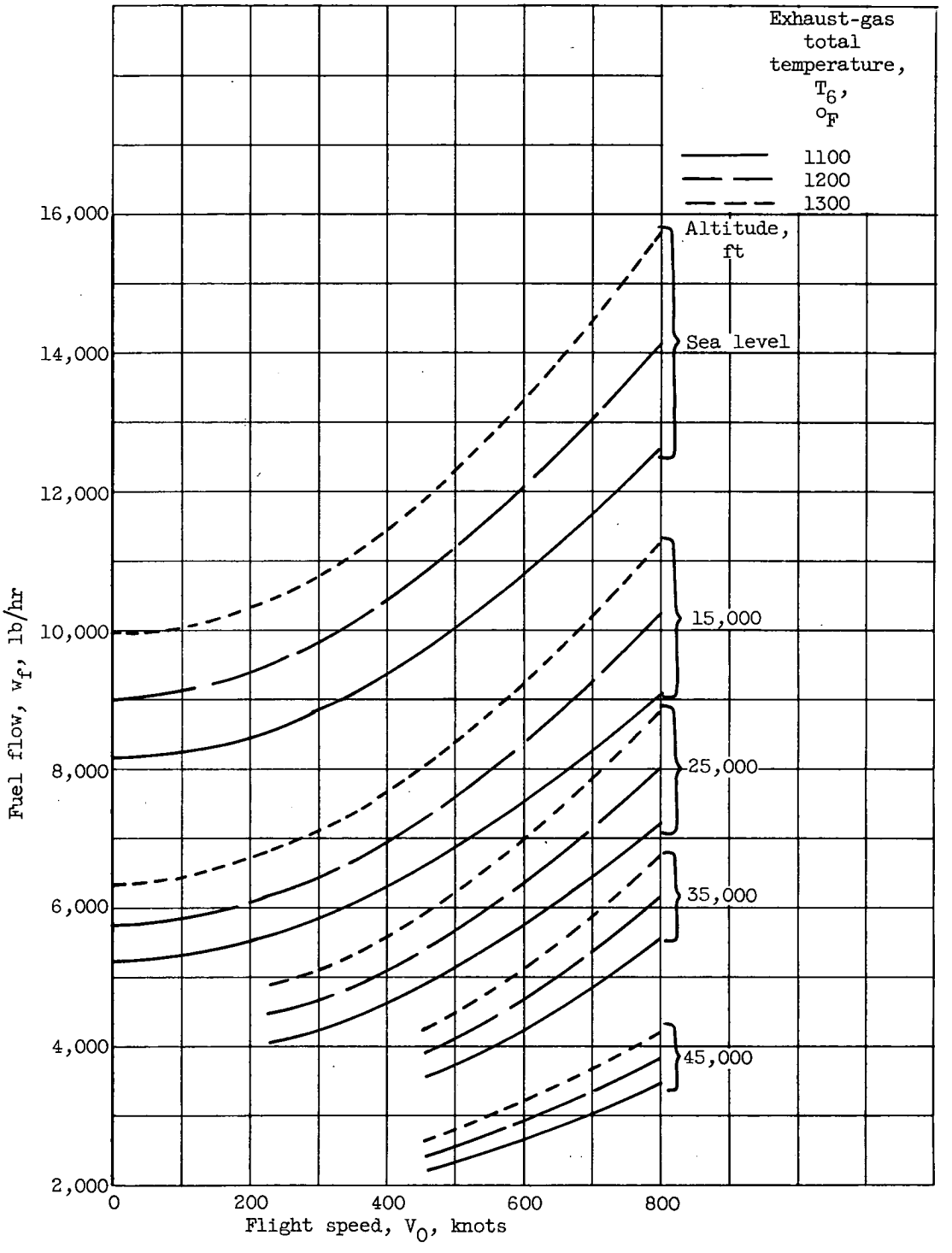


(b) Fuel flow.

Figure 19. - Continued. Low-altitude performance using JP-4 fuel. Engine speed, 6100 rpm; NACA standard atmosphere; 100-percent ram-pressure recovery.

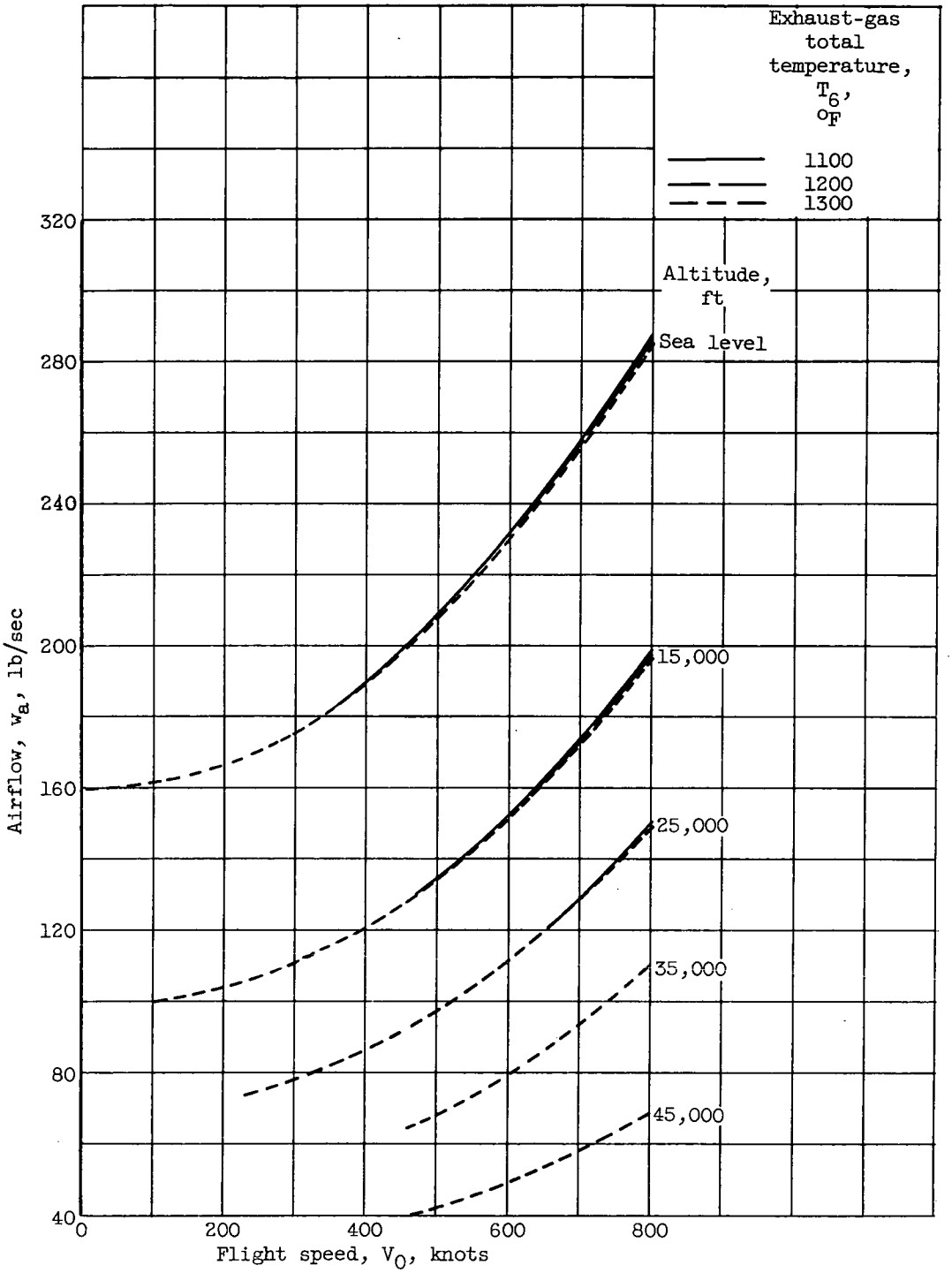


(c) Airflow.

Figure 19. - Concluded. Low-altitude performance using JP-4 fuel. Engine speed, 6100 rpm; NACA standard atmosphere; 100-percent ram-pressure recovery.

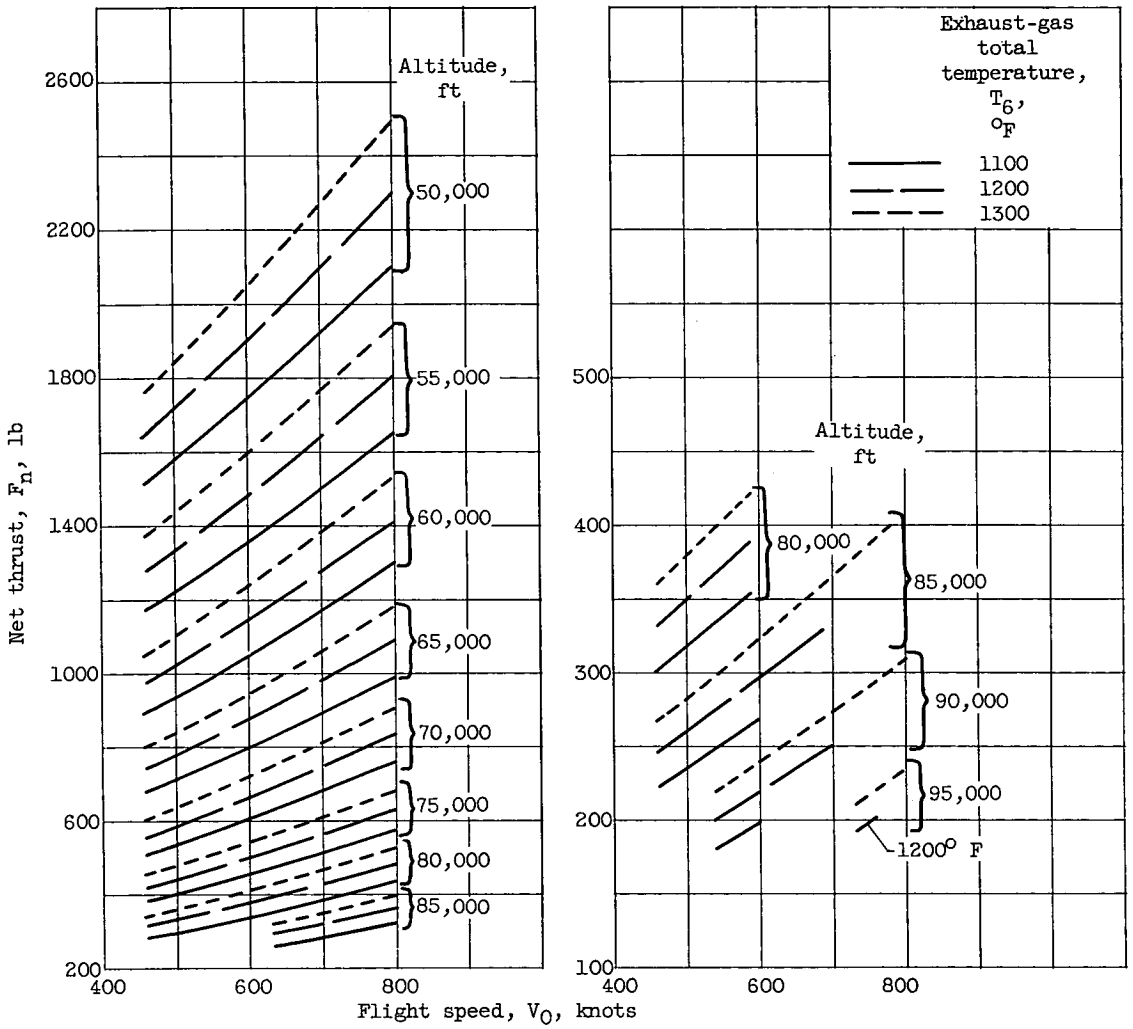


(a) Net thrust using JP-4 fuel.

(b) Net thrust using gaseous-hydrogen fuel.

Figure 20. - High-altitude performance. Engine speed, 6100 rpm; NACA standard atmosphere; 100-percent ram-pressure recovery.

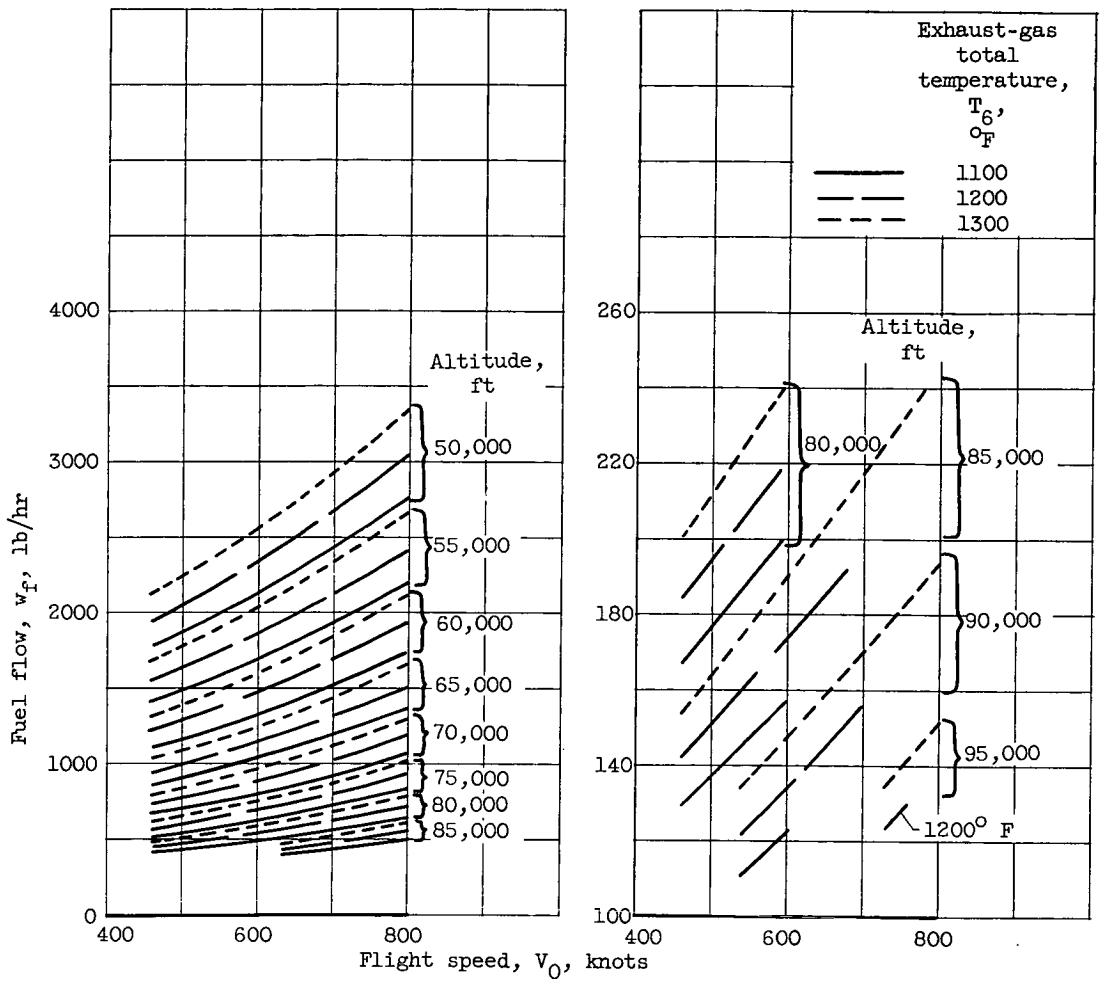


(c) Fuel flow using JP-4 fuel.

(d) Fuel flow using gaseous-hydrogen fuel.

Figure 20. - Continued. High-altitude performance. Engine speed, 6100 rpm; NACA standard atmosphere; 100-percent ram-pressure recovery.

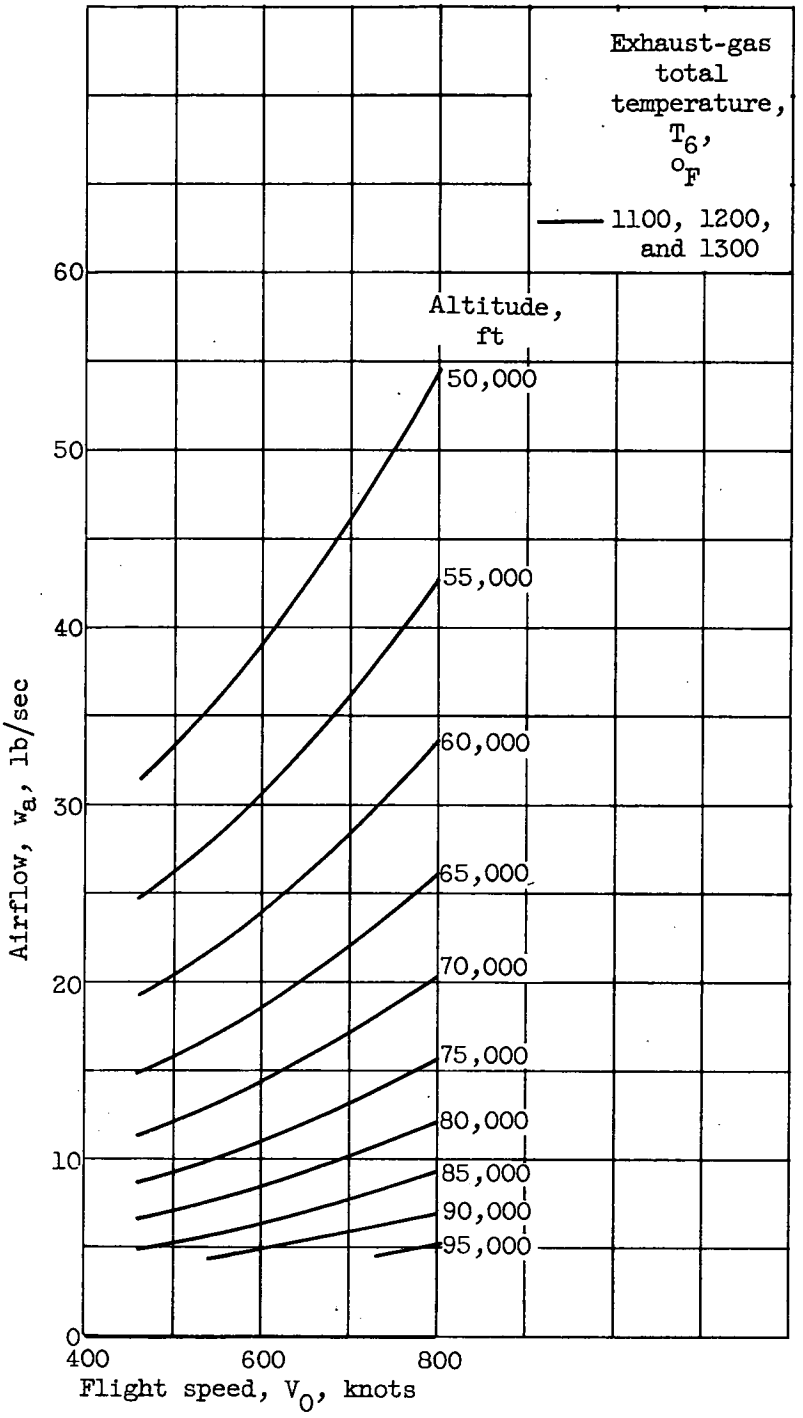


(e) Airflow for both JP-4 and gaseous-hydrogen fuels.

Figure 20. - Concluded. High-altitude performance. Engine speed, 6100 rpm; NACA standard atmosphere; 100-percent ram-pressure recovery.

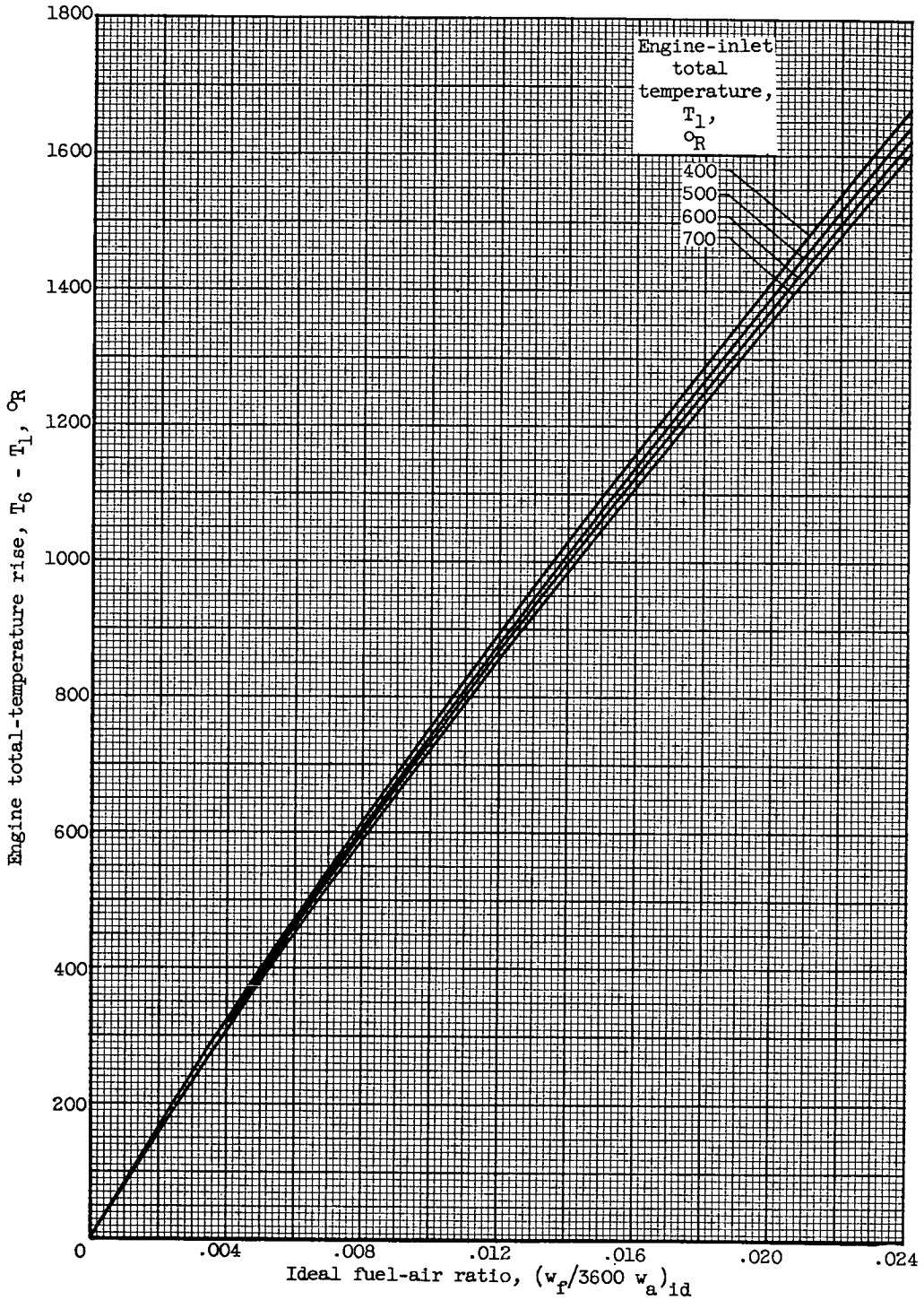


(a) JP-4 fuel. Lower heating value, 18,700 Btu/lb; hydrogen-carbon ratio, 0.171.

Figure 21. - Ideal fuel-air ratio.

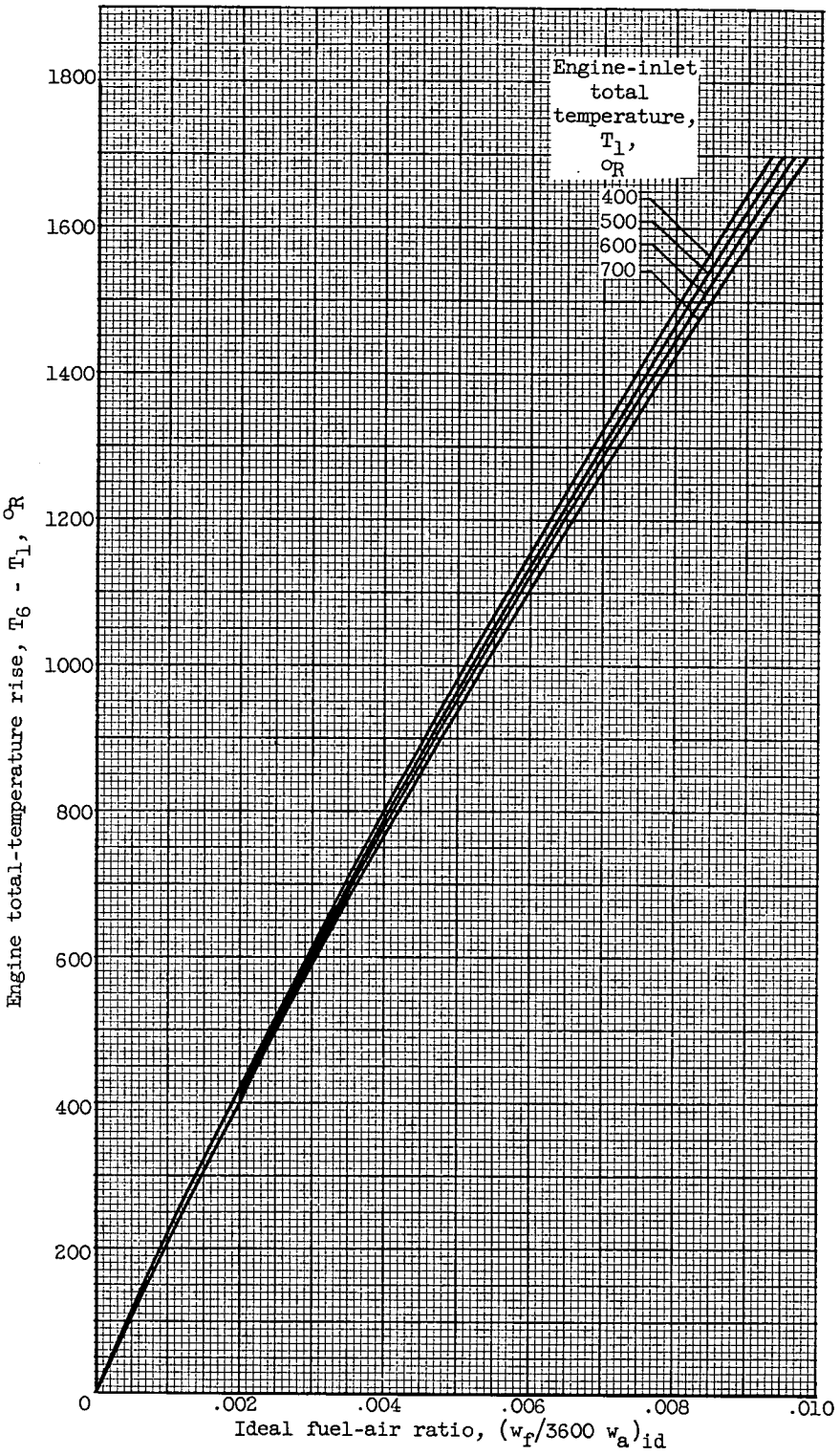


(b) Gaseous-hydrogen fuel. Lower heating value, 51,570 Btu/lb.

Figure 21. - Concluded. Ideal fuel-air ratio.

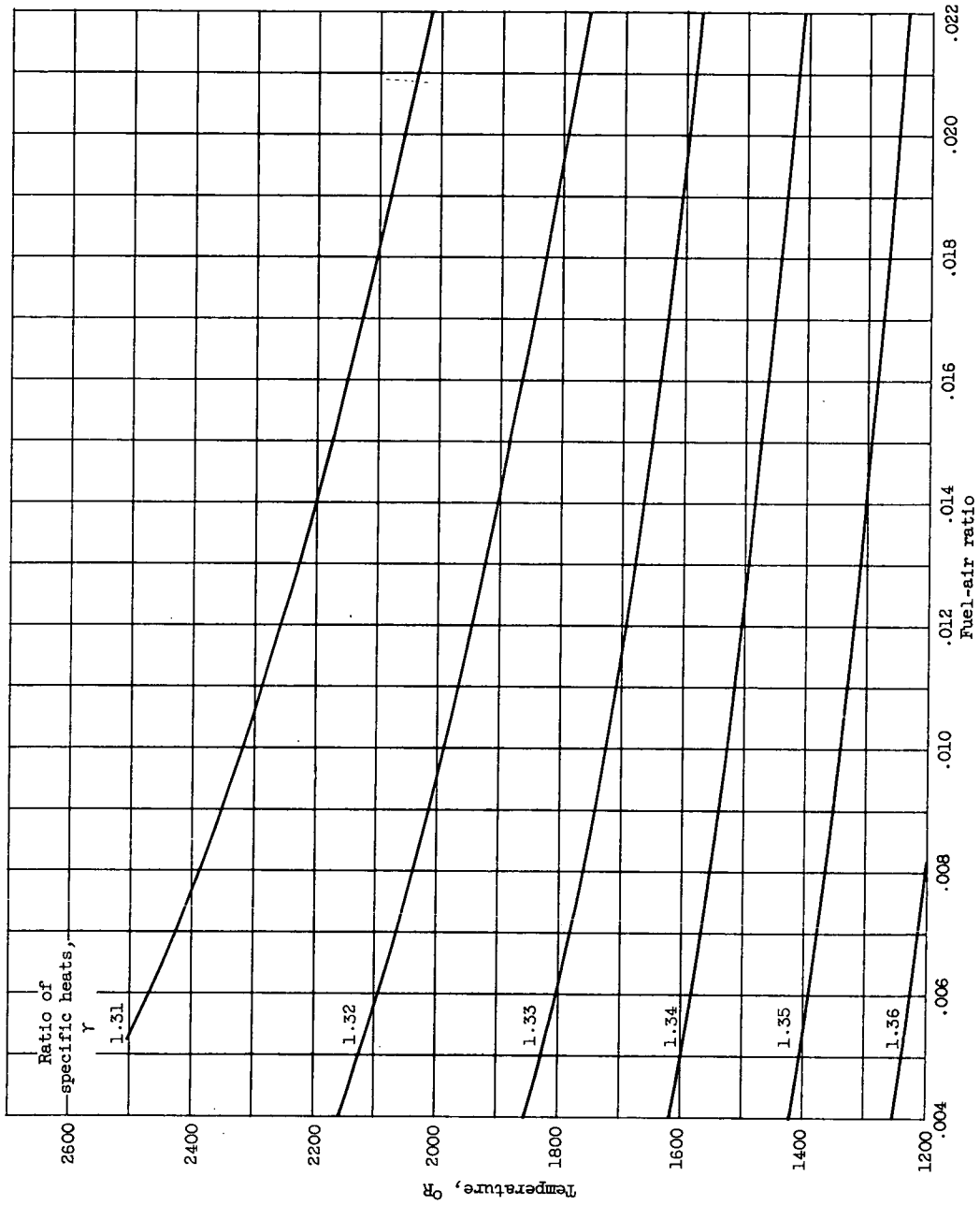


(a) JP-4 fuel.

Figure 22. - Ratio of specific heats of exhaust gas.

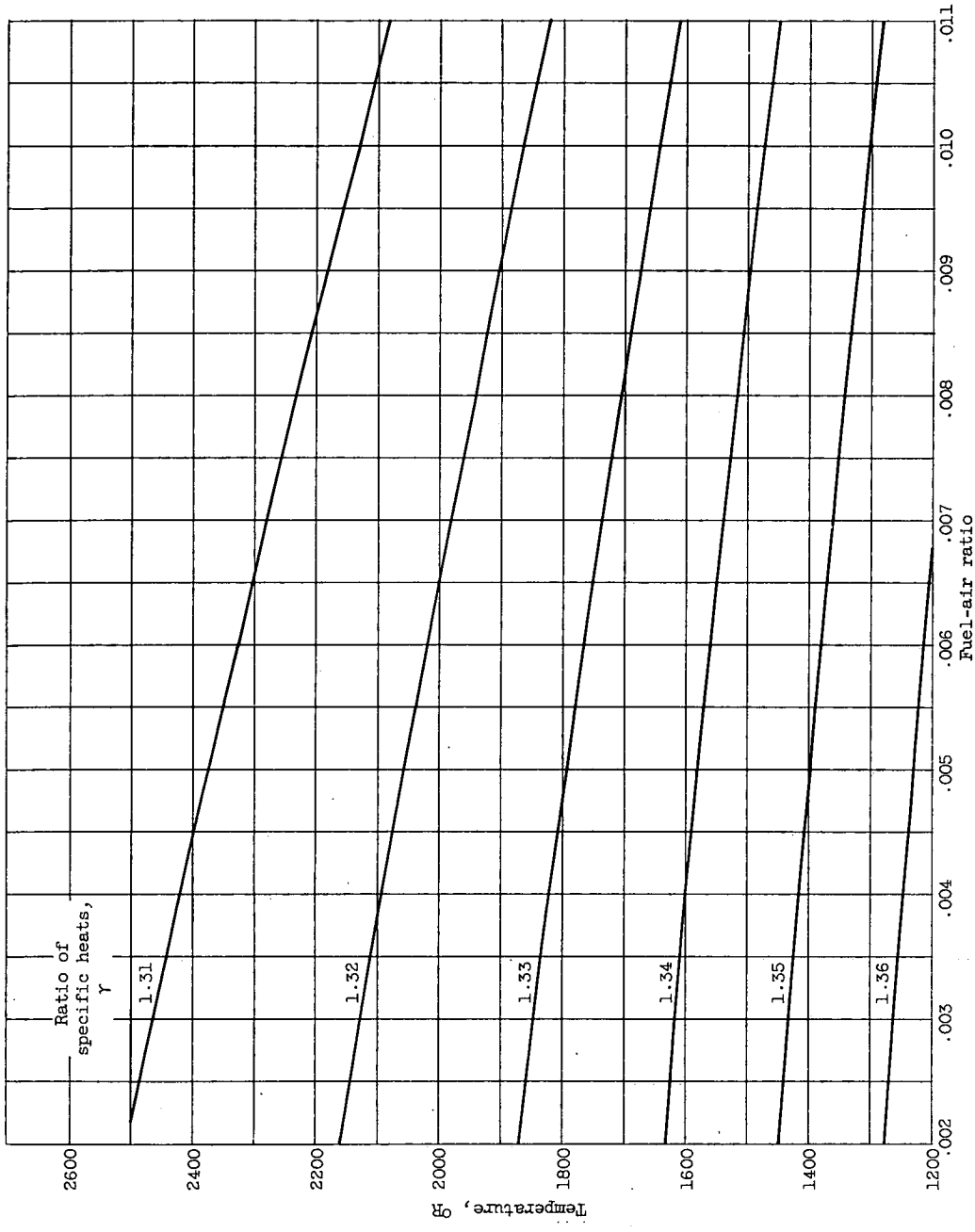


(b) Gaseous-hydrogen fuel.

Figure 22. - Concluded. Ratio of specific heats of exhaust gas.

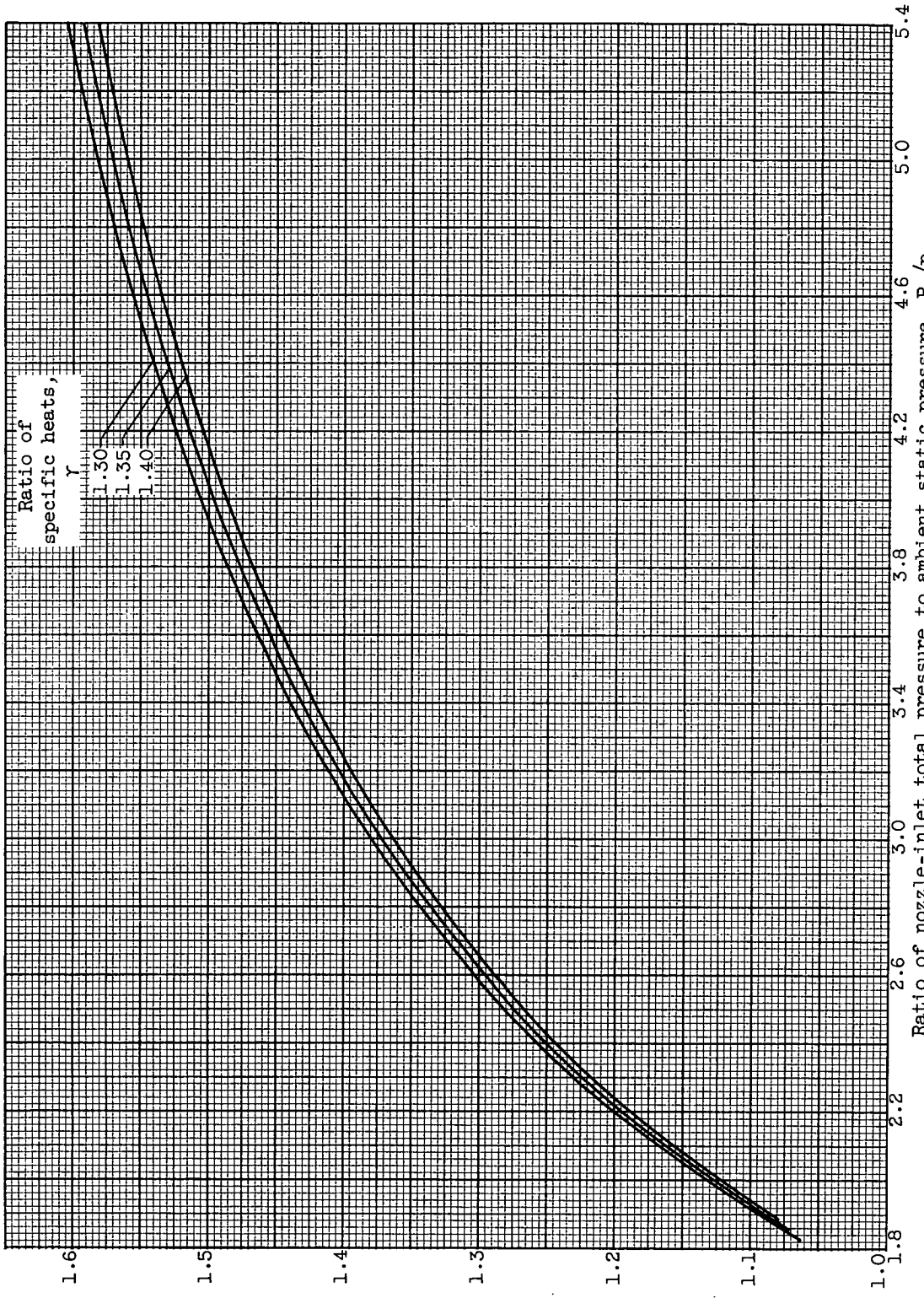


Figure 23. - Effective velocity parameter.

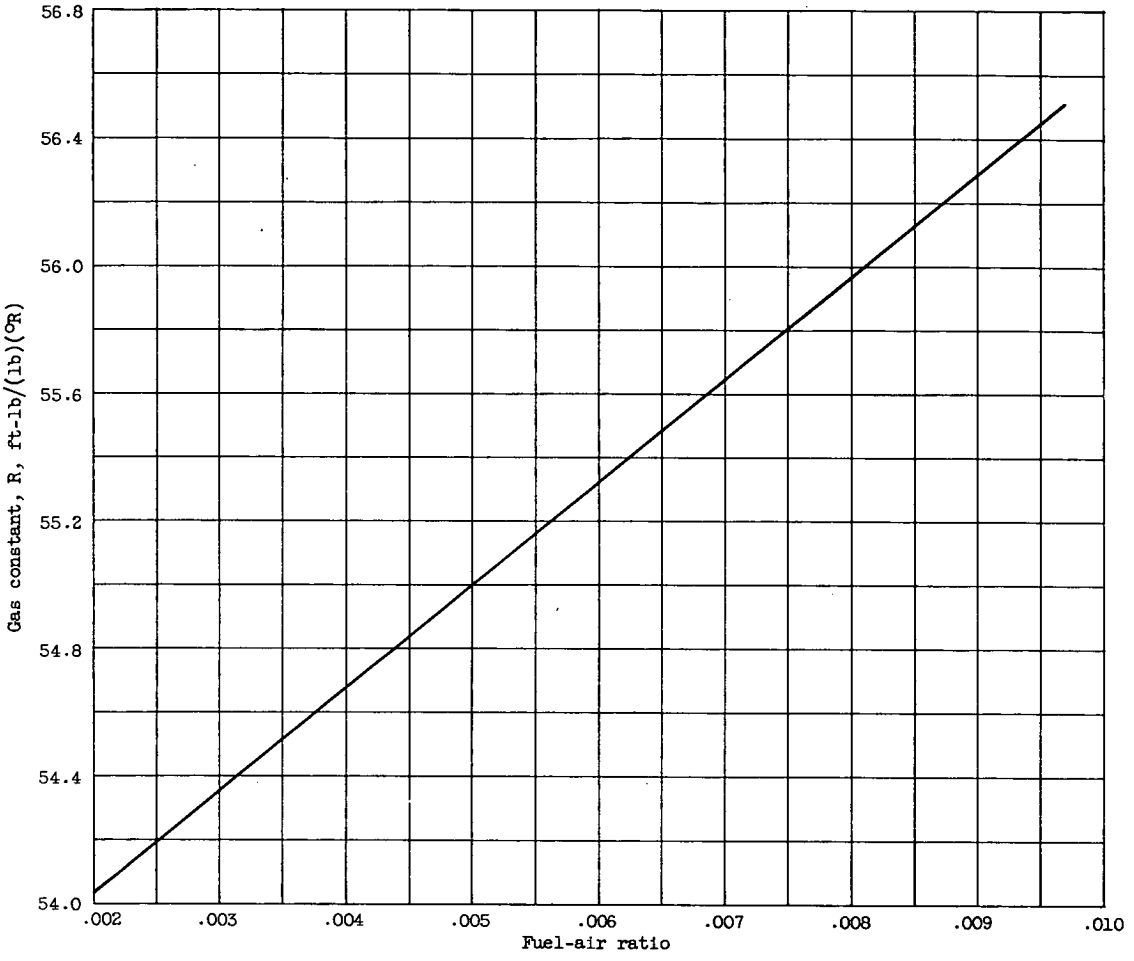


Figure 24. - Gas constant for gaseous-hydrogen fuel.

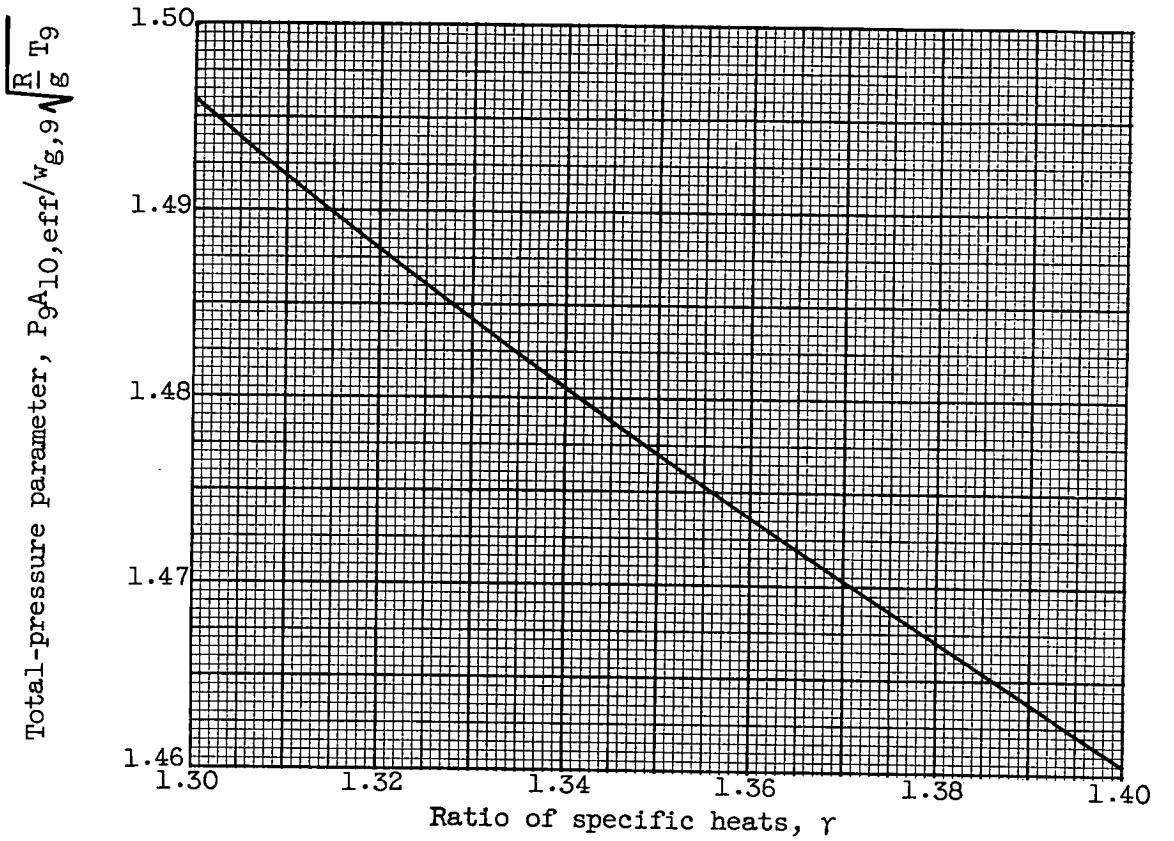


Figure 25. - Total-pressure parameter for choked exhaust-nozzle flow.